

Preprint of an article published in International Journal of Pattern Recognition and Artificial Intelligence (<https://www.worldscientific.com/worldscinet/ijprai>)

© World Scientific Publishing Company

DOI: 10.1142/S0218001421510083

Upper Bounding the Graph Edit Distance Based on Rings and Machine Learning

David B. Blumenthal*

*Technical University of Munich
Chair of Experimental Bioinformatics
Freising, Germany
david.blumenthal@wzw.tum.de*

Johann Gamper

*Free University of Bozen-Bolzano
Faculty of Computer Science
Bozen, Italy
gamper@inf.unibz.it*

Sébastien Bogleux

*Normandie Université
ENSICAEN, UNICAEN, CNRS, GREYC
Caen, France
sebastien.bogleux@unicaen.fr*

Luc Brun

*Normandie Université
ENSICAEN, UNICAEN, CNRS, GREYC
Caen, France
luc.brun@ensicaen.fr*

The graph edit distance (GED) is a flexible distance measure which is widely used for inexact graph matching. Since its exact computation is \mathcal{NP} -hard, heuristics are used in practice. A popular approach is to obtain upper bounds for GED via transformations to the linear sum assignment problem with error-correction (LSAPE). Typically, local structures and distances between them are employed for carrying out this transformation, but recently also machine learning techniques have been used. In this paper, we formally define a unifying framework LSAPE-GED for transformations from GED to LSAPE. We also introduce rings, a new kind of local structures designed for graphs where most information resides in the topology rather than in the node labels. Furthermore, we propose two new ring based heuristics RING and RING-ML , which instantiate LSAPE-GED using the traditional and the machine learning based approach for transforming GED to LSAPE, respectively. Extensive experiments show that using rings for upper bounding GED significantly improves the state of the art on datasets where most information

*Corresponding author.

2 *D.B. Blumenthal, J. Gamper, S. Bougleux & L. Brun*

resides in the graphs' topologies. This closes the gap between fast but rather inaccurate LSAP based heuristics and more accurate but significantly slower GED algorithms based on local search.

Keywords: Graph edit distance; graph matching; graph similarity search; machine learning.

1. Introduction

Labeled graphs can be used for modeling various kinds of objects, such as chemical compounds, images, and molecular structures. Because of this flexibility, they have received increasing attention over the past years. One task researchers have focused on is the following: Given a database \mathcal{G} that contains labeled graphs, find all graphs $G \in \mathcal{G}$ that are sufficiently similar to a query graph H or find the k graphs from \mathcal{G} that are most similar to H .^{20,51} Being able to quickly answer graph similarity queries is crucial for the development of performant pattern recognition techniques in various application domains,⁴⁹ such as keyword spotting in handwritten documents⁴⁸ and cancer detection.³⁵

For answering graph similarity queries, a distance measure between two labeled graphs G and H has to be defined. A very flexible, sensitive and therefore widely used measure is the graph edit distance (GED), which is defined as the minimum cost of an edit path between G and H .¹⁴ An edit path is a sequence of graphs starting at G and ending at a graph that is isomorphic to H such that each graph on the path can be obtained from its predecessor by applying one of the following edit operations: adding or deleting an isolated node or an edge, and relabelling an existing node or edge. Each edit operation comes with an associated non-negative edit cost, and the cost of an edit path is defined as the sum of the costs of its edit operations. GED inherits metric properties from the underlying edit costs.²⁴ For instance, if \mathfrak{G} is the domain of graphs with real-valued node and edge labels and the edit costs are defined as the Euclidean distances between the labels, then GED is a metric on \mathfrak{G} .

GED is mainly used in settings where we have to answer fine-grained similarity queries for (possibly very many) rather small graphs. For instance, this is the case in keyword spotting in handwritten documents, cancer detection, and drug discovery.⁴⁹ If the graphs are larger, faster approaches such as embedding the graphs into vector spaces and then comparing their vector representations may be used.^{20,51} The drawback of these faster techniques is that a substantial part of the local information encoded in the original graphs is lost when embedding them into vector spaces. Whenever this information loss is intolerable, it is advisable to compare the graphs directly in the graph space — and one of the most commonly used distance measure for doing so is GED.

1.1. Related work

Computing GED is a very difficult problem. It has been shown that the problem of computing GED is \mathcal{NP} -hard even for uniform edit costs,⁵² and \mathcal{APX} -hard for metric

edit costs.³² Even worse: since, by definition of GED, it holds that $\text{GED}(G, H) = 0$ just in case G and H are isomorphic, approximating GED within any approximation ratio is \mathcal{GI} -hard. These theoretical complexities are mirrored by the fact that, in practice, no available exact algorithm can reliably compute GED on graphs with more than 16 nodes.⁸

Because of GED’s complexity, research has mainly focused on heuristics.³ The development of heuristics was particularly triggered by the presentation of the algorithms **BP**³⁸ and **STAR**,⁵² which use transformations to the linear sum assignment problem with error correction (LSAPE) — a variant of the linear sum assignment problem (LSAP) where rows and columns may also be inserted and deleted — to compute upper bounds for GED. **BP** and **STAR** work as follows: First, the nodes of the input graphs are associated with local structures composed of branches (**BP**) or stars (**STAR**), respectively. The branch of a node is defined as the node itself together with its incident edges, whereas the star additionally contains the incident edges’ terminal nodes. Then, suitable distance measures between, respectively, branches and stars are used to populate instances of LSAPE whose rows and columns correspond to the input graphs’ nodes. Finally, the solution of the LSAPE instance is interpreted as an edit path whose cost is returned as upper bound for GED.

Following **BP** and **STAR**, many similar algorithms have been proposed. Like **BP**, the algorithms **BRANCH-UNI**,⁵⁵ **BRANCH-FAST**,⁷ and **BRANCH**⁷ use branches as local structures, but use slightly different distance measures between the branches that allow to also derive lower bounds. The main disadvantage of these algorithms as well as of **BP** and **STAR** is that, due to the very narrow locality of the local structures, they yield unsatisfactorily loose upper bounds on datasets where the nodes only carry little information and most information instead resides in the graphs’ topologies.

In order to produce tight upper bounds even if there is little information on the nodes, the algorithms **SUBGRAPH**¹⁵ and **WALKS**²¹ associate the nodes with larger local structures — namely, subgraphs of fixed radiuses and sets of walks of fixed lengths. The drawback of **SUBGRAPH** is that it runs in polynomial time only if the input graphs have constantly bounded maximum degrees. **WALKS** avoids this blowup, but only models constant edit costs and uses local structures that may contain redundant information due to multiple inclusions of nodes and edges. It has also been suggested to tighten the upper bounds by incorporating node centrality measures into the LSAPE instances.^{41, 47}

Recently, two machine learning based heuristics for GED have been proposed, which are closely related to the aforementioned LSAPE based approaches. The algorithm **PREDICT**⁴² calls **BP** to compute an LSAPE instance and uses statistics of the LSAPE instance to define feature vectors for all node assignments. **PREDICT** then trains a support vector classifier (SVC) to predict if a node edit assignment is contained in an optimal edit path. The algorithm **NGM**¹⁷ defines feature vectors of node substitutions in terms of the input graphs’ node labels and node degrees. Given a set of optimal edit paths, **NGM** trains a deep neural network (DNN) to output

a value close to 0 if the substitution is predicted to be in an optimal edit path, and close to 1, otherwise. The output is used to populate an instance of the linear sum assignment problem (LSAP), whose solution induces an upper bound for GED. NGM does not support node insertions and deletions and can hence be used only for equally sized graphs. Moreover, it ignores edge labels and assumes that the node labels are real-valued vectors. PREDICT works for general graphs but does not yield an upper bound for GED.

Not all heuristics for GED build upon transformations to LSAP. For instance, further machine learning based algorithms have been suggested in Ref. 30, 29, 2. In Ref. 30, Bayesian networks are employed to learn probabilities $\Pr(\text{GED}(G, H) \leq \tau)$, which are then used to approximatively answer graph similarity queries. In Ref. 29, 2, graph neural networks are used to learn GED estimates from ground truth training data. All of these approaches are designed for uniform edit costs only, i. e., for the case where all edit operations have the same cost. This assumption simplifies the concept of GED, but is not met in most real-world application scenarios where GED is used.⁴⁹ Moreover, no assignments between the nodes of the compared graphs are computed, and the returned estimates for GED are not guaranteed to be upper or lower bounds.

The tightest lower bounds for GED are computed by heuristics based on linear programming.^{24, 27, 28} These algorithms formulate the problem of computing GED as integer linear programs and call solvers such as CPLEX²³ or Gurobi²² to solve the continuous relaxations. Subsequently, the costs of the optimal continuous solutions are returned as lower bounds for GED. For uniform edit costs, heuristics based on graph partitioning also yield good lower bounds.^{25, 31, 53–55} In these approaches, one of the two input graphs is partitioned into small subgraphs. Subsequently, it is counted how many of the small subgraphs are not subgraph-isomorphic to the other input graph. If the edit costs are uniform, this count is a lower bound for GED.

For upper bounding GED, LSAP based heuristics are still among the most competitive approaches, as shown in a recent experimental evaluation survey.³ In terms of accuracy, they are outperformed only by algorithms using variants of local search.^{6, 9–11, 18, 19, 40, 44, 52} However, these algorithms are much slower than LSAP based heuristics. Among local search based approaches, IPFP is the best performing algorithm.^{6, 9–11, 18} In Ref. 3, it is shown empirically that, on six benchmark datasets, IPFP’s upper bound exceeds the best available lower bounds, and hence the true GED, by at most 4.23%.

1.2. Contributions

In this paper, we formally describe a paradigm LSAP-GED that generalizes all existing transformations from GED to LSAP. Classical instantiations of LSAP-GED such as BP, STAR, BRANCH-UNI, BRANCH-FAST, BRANCH, SUBGRAPH, and WALKS use local structures and distance measures between them for the transformation. We introduce a partial order that compares classical instantiations in terms of the employed local

structures’ topological information content, and use it to systematically compare BP, STAR, BRANCH-UNI, BRANCH-FAST, BRANCH, SUBGRAPH, and WALKS.

We also suggest a new, machine learning based approach inspired by the algorithms PREDICT and NGM: During training, feature vectors for all possible node assignments are constructed and a machine learning framework is trained to output a value close to 0 if a node assignment is predicted to be contained in an optimal edit path, and a value close to 1, otherwise. At runtime, the output of the machine learning framework is fed into an LSAPE instance.

As mentioned above, PREDICT and NGM use SVCs or DNNs as their machine learning frameworks. They hence require training data that consists of node assignments some of which are and some of which are not contained in optimal edit paths. We argue that constructing such training data in a clean way is computationally infeasible. In order to overcome this problem, we suggest to use one class support vector machines (1-SVM) instead of SVCs and DNNs.

Next, we present a new kind of local structures—namely, rings of fixed sizes. Rings are sequences of disjoint node and edge sets at fixed distances from a root node. Like the local structures used by SUBGRAPH and WALKS, rings are primarily designed for graphs where most information is encoded in the topologies rather than in the node labels. Using the partial order introduced before, we prove that rings indeed capture more topological information than the local structures used by the baseline approaches BP, STAR, BRANCH-UNI, BRANCH-FAST, and BRANCH. The advantage of rings w. r. t. subgraphs is that rings can be processed in polynomial time. The advantage w. r. t. walks is that rings model general edit costs and avoid redundancies due to multiple inclusions of nodes and edges.

Subsequently, we propose RING and RING-ML, two instantiations of LSAPE-GED that make crucial use of rings. RING adopts the classical approach, i. e., carries out the transformation via a suitably defined ring distance measure. In contrast to that, RING-ML uses rings to construct feature vectors for the node assignments and then uses machine learning techniques to carry out the transformation.

An extensive empirical evaluation shows that RING-ML shows very promising potential and that, among all instantiations of LSAPE-GED, RING produces the tightest upper bound for GED, especially on datasets where most information is encoded in the graphs’s topologies. The newly proposed heuristic RING hence closes the gap between existing instantiations of LSAPE-GED and the tighter but much slower local search algorithm IPFP. In sum, our paper contains the following contributions:

- We formalize the paradigm LSAPE-GED and the classical, local structure distance based approach for transforming GED to LSAPE, and show how to use machine learning for this purpose (Section 3).
- We argue that 1-SVMs instead of classifiers such as DNNs or SVCs should be used in machine learning based transformations to LSAPE (Section 3).
- We introduce rings, a new kind of local structures designed to yield tight upper bounds if most information is encoded in the graphs’ topologies rather

6 *D.B. Blumenthal, J. Gamper, S. Bougleux & L. Brun*

than in the node labels (Section 4).

- We present two new **LSAPE-GED** instantiations **RING** and **RING-ML** (Section 5).
- We report results of extensive experiments (Section 6).

This paper extends the results presented in Ref. 4, where we informally described **LSAPE-GED**, introduced rings, and presented and preliminarily evaluated **RING**. In particular, the following contributions are new: formal definition of **LSAPE-GED**, the use of machine learning techniques in general and 1-SVMs in particular for transforming GED to **LSAPE**, the algorithm **RING-ML**, and additional experiments.

The rest of the paper is organized as follows: In Section 2, we introduce concepts and notations. In Sections 3 to 6, we present our contributions. Section 7 concludes the paper.

2. Preliminaries

We consider undirected labeled graphs $G = (V^G, E^G, \ell_V^G, \ell_E^G)$ from a domain of graphs \mathfrak{G} . V^G and E^G are sets of nodes and edges, Σ_V and Σ_E are label alphabets, and $\ell_V^G : V^G \rightarrow \Sigma_V$ and $\ell_E^G : E^G \rightarrow \Sigma_E$ are labeling functions. $\mathfrak{I} := \{(G, u) \mid G \in \mathfrak{G} \wedge u \in (V^G \cup \epsilon)\}$ is the set of all graph-node incidences and $\mathfrak{A} := \{(G, H, u, v) \mid (G, u) \in \mathfrak{I} \wedge (H, v) \in \mathfrak{I} \wedge (u \neq \epsilon \vee v \neq \epsilon)\}$ is the set of all node assignments. The symbol ϵ denotes dummy nodes and edges as well as their labels. For each $N \in \mathbb{N}_{\geq 1}$, we define $[N] := \{n \in \mathbb{N}_{\geq 1} \mid n \leq N\}$.

An edit path from a graph G to a graph H is a sequence of edit operations that transforms G into H . There are six edit operations: Substituting a node or an edge from G by a node or an edge from H , deleting an isolated node or an edge from G , and inserting an isolated node or an edge between two existing nodes into H . Each edit operation o comes with an edit cost $c(o)$ defined in terms of edit cost functions $c_V : \Sigma_V \cup \{\epsilon\} \times \Sigma_V \cup \{\epsilon\} \rightarrow \mathbb{R}_{\geq 0}$ and $c_E : \Sigma_E \cup \{\epsilon\} \times \Sigma_E \cup \{\epsilon\} \rightarrow \mathbb{R}_{\geq 0}$ (cf. Table 1), which respect $c_V(\alpha, \alpha) = 0$ and $c_E(\beta, \beta) = 0$ for all $\alpha \in \Sigma_V \cup \{\epsilon\}$ and all $\beta \in \Sigma_E \cup \{\epsilon\}$. The cost of an edit path $P = (o_i)_{i=1}^r$ is defined as $c(P) := \sum_{i=1}^r c(o_i)$.

Definition 1 (GED). Let $\Psi(G, H)$ be the set of all edit paths from a graph G to a graph H . Then graph edit distance is defined as $\text{GED}(G, H) := \min_{P \in \Psi(G, H)} c(P)$.

Definition 1 is very intuitive but algorithmically inaccessible, because for recognizing an edit path as such, one has to solve the graph isomorphism problem. Thus, algorithms for GED use an alternative definition based on the concept of error-correcting matchings or node maps.^{8, 11, 14}

Definition 2 (Node Map). Let G and H be graphs. A relation $\pi \subseteq (V^G \cup \{\epsilon\}) \times (V^H \cup \{\epsilon\})$ is called node map between G and H if and only if $|\{v \mid v \in (V^H \cup \{\epsilon\}) \wedge (u, v) \in \pi\}| = 1$ holds for all $u \in V^G$ and $|\{u \mid u \in (V^G \cup \{\epsilon\}) \wedge (u, v) \in \pi\}| = 1$ holds for all $v \in V^H$. We write $\pi(u) = v$ just in case $(u, v) \in \pi$ and $u \neq \epsilon$, and

Table 1. Notation table.

| syntax | semantics |
|---------------------------------|---|
| \mathfrak{G} | graphs on label alphabets Σ_V and Σ_E |
| \mathfrak{J} | graph-node incidences in \mathfrak{G} |
| \mathfrak{A} | node assignments between graphs in \mathfrak{G} |
| $c_V(\ell_V^G(u), \ell_V^H(v))$ | cost of substituting $u \in V^G$ by $v \in V^H$ |
| $c_E(\ell_E^G(e), \ell_E^H(f))$ | cost of substituting $e \in E^G$ by $f \in E^H$ |
| $c_V(\ell_V^G(u), \epsilon)$ | cost of deleting $u \in V^G$ |
| $c_E(\ell_E^G(e), \epsilon)$ | cost of deleting $e \in E^G$ |
| $c_V(\epsilon, \ell_V^H(v))$ | cost of inserting $v \in V^H$ |
| $c_E(\epsilon, \ell_E^H(f))$ | cost of inserting $f \in E^H$ |
| $\Pi(G, H)$ | node maps between graphs G and H |
| $c(\pi)$ | node map π 's induced edit cost |
| $\Pi(\mathbf{C})$ | feasible solutions for LSAP instance \mathbf{C} |

$\pi^{-1}(v) = u$ just in case $(u, v) \in \pi$ and $v \neq \epsilon$. $\Pi(G, H)$ denotes the set of all node maps between G and H .

A node map $\pi \in \Pi(G, H)$ specifies for all nodes $u \in V^G$ and $v \in V^H$ and all edges $e = (u_1, u_2) \in E^G$ and $f = (v_1, v_2) \in E^H$ if they are substituted, deleted, or inserted: If $\pi(u) = v$, the node u is substituted by v ; if $\pi(u) = \epsilon$, u is deleted; and if $\pi^{-1}(v) = \epsilon$, v is inserted. Similarly, if $(\pi(u_1), \pi(u_2)) = (v_1, v_2)$, the edge e is substituted by f ; if $(\pi(u_1), \pi(u_2)) \notin E^H$, e is deleted; and if $(\pi^{-1}(v_1), \pi^{-1}(v_2)) \notin E^G$, f is inserted. A node map $\pi \in \Pi(G, H)$ hence induces an edit path from G to H . It has been shown that, for computing GED, it suffices to consider edit paths induced by node maps.^{8, 11, 14, 36}

Theorem 1 (Alternative Definition of GED). *Let G and H be graphs and $c(\pi)$ be the cost of the edit path induced by a node map $\pi \in \Pi(G, H)$. Then, under mild constraints on the edit costs that can be assumed to hold w. l. o. g. (cf. Ref. 8 for details), it holds that $\text{GED}(G, H) = \min_{\pi \in \Pi(G, H)} c(\pi)$.*

Since node maps are much easier objects to work with than edit paths, Theorem 1 renders GED algorithmically accessible. In particular, it implies that each node map induces an upper bound for GED. This observation is used by approximative methods for GED, which heuristically compute a node map that induces a tight upper bound. For finding such a node map, many heuristics^{7, 15, 21, 38, 41, 47, 52, 55} use the linear sum assignment problem with error correction (LSAPE)^{12, 13} — although usually not under this name, since LSAP was formalized after the presentation of most of these heuristics.

Definition 3 (LSAPE). Let $\mathbf{C} = (c_{i,k}) \in \mathbb{R}^{(n+1) \times (m+1)}$ be a matrix with $c_{n+1, m+1} = 0$. A relation $\pi \subseteq [n+1] \times [m+1]$ is a feasible LSAP solution for \mathbf{C} , if and only if $|\{k \mid k \in [m+1] \wedge (i, k) \in \pi\}| = 1$ holds for all $i \in [n]$ and

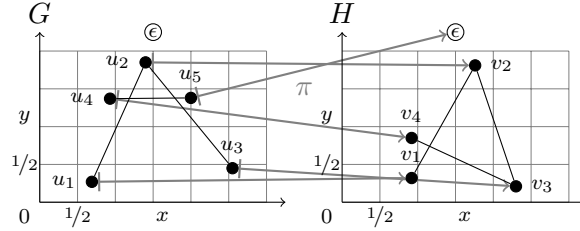


Fig. 1. Two graphs G and H from the LETTER dataset and a node map π .

$|\{i \mid i \in [n+1] \wedge (i, k) \in \pi\}| = 1$ holds for all $k \in [m]$. We write $\pi(i) = k$ if $(i, k) \in \pi$ and $i \neq n+1$; and $\pi^{-1}(k) = i$ if $(i, k) \in \pi$ and $k \neq m+1$. The set of all feasible LSAP solutions for \mathbf{C} is denoted by $\Pi(\mathbf{C})$. The cost of a feasible solution $\pi \in \Pi(\mathbf{C})$ is defined as $\mathbf{C}(\pi) := \sum_{(i,k) \in \pi} c_{i,k}$. The set of all optimal LSAP solutions for \mathbf{C} is defined as $\Pi^*(\mathbf{C}) := \arg \min_{\pi \in \Pi(\mathbf{C})} \mathbf{C}(\pi)$.

An optimal LSAP solution $\pi \in \Pi^*(\mathbf{C})$ can be computed in $\mathcal{O}(\min\{n, m\}^2 \max\{n, m\})$ time.¹³ Once one optimal solution has been found, for each $s \in [|\Pi^*(\mathbf{C})|]$, a solution set $\Pi_s^*(\mathbf{C}) \subseteq \Pi^*(\mathbf{C})$ of size s can be enumerated in $\mathcal{O}(nm\sqrt{n+m} + s \log(n+m))$ time.⁵⁰ Greedy suboptimal solutions can be computed in $\mathcal{O}(nm)$ time.⁴³

Node maps and feasible solutions for LSAP are closely related. Consider graphs G and H and an LSAP instance $\mathbf{C} \in \mathbb{R}^{(|V^G|+1) \times (|V^H|+1)}$. Definition 2 and Definition 3 imply that we can identify the set $\Pi(G, H)$ of all node maps between G and H with the set $\Pi(\mathbf{C})$ of all feasible LSAP solutions for \mathbf{C} : For all $i \in [|V^G|]$ and all $k \in [|V^H|]$, we associate \mathbf{C} 's i^{th} row with the node $u_i \in V^G$ and \mathbf{C} 's k^{th} column with the node $v_k \in V^H$. The last row and the last column of \mathbf{C} are associated with the dummy node ϵ . Then, each feasible LSAP solution π for \mathbf{C} yields an upper bound for $\text{GED}(G, H)$ — namely, the cost $c(\pi)$ of the edit path induced by π 's interpretation as a node map.

Example 1 (Most Important Definitions). The graphs G and H shown in Figure 1 are taken from the LETTER dataset and represent distorted letter drawings.³⁷ Nodes are labeled with two-dimensional, non-negative Euclidean coordinates. Edges are unlabeled. Hence, we have $\Sigma_V = \mathbb{R}_{\geq 0}^2$ and $\Sigma_E = \{1\}$. In Ref. 39, the following edit cost functions are suggested: $c_E(1, \epsilon) := c_E(\epsilon, 1) := 0.425$, $c_V(\alpha, \alpha') := 0.75 \|\alpha - \alpha'\|$, and $c_V(\alpha, \epsilon) := c_V(\epsilon, \alpha) := 0.675$, where $\|\cdot\|$ is the Euclidean norm. The node map $\pi \in \Pi(G, H)$ induces the following edit operations: substitutions of the nodes u_i by the nodes v_i , for all $i \in [4]$, deletion of node u_5 , substitutions of the edges (u_i, u_{i+1}) by the edges (v_i, v_{i+1}) , for all $i \in [2]$, deletion of the edge (u_4, u_5) , insertion of the edge (v_3, v_4) . By summing the induced edit costs, we obtain that π 's induced edit path has cost $c(\pi) = 2.574$ and hence $\text{GED}(G, H) \leq 2.574$.

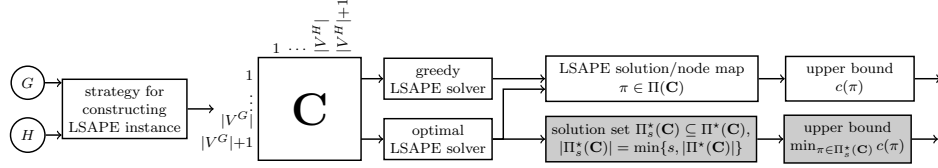


Fig. 2. The paradigm LSAPe-GED. Our alternative solution strategy is displayed in grey.

3. LSAPe Based Upper Bounds for GED

In this section, we present the paradigm LSAPe-GED (Section 3.1). We show that existing LSAPe based approaches for upper bounding GED are instances of LSAPe-GED and define a partial order in terms of their local structures' topological information content (Section 3.2). Subsequently, we present a new machine learning technique to create LSAPe instances (Section 3.3). We also identify a problem that occurs if classifiers such as SVCs or DNNs are used for creating the LSAPe instances, and suggest that one should resort to 1-SVMs to overcome it.

3.1. Overall structure of the paradigm LSAPe-GED

Figure 2 shows how to use LSAPe for upper bounding GED: Given two graphs G and H , first an LSAPe instance $\mathbf{C} \in \mathbb{R}^{(|V^G|+1) \times (|V^H|+1)}$ is constructed. Different strategies can be used for the construction, which are detailed in Section 3.2 and Section 3.3. Subsequently, existing LSAPe based heuristics call a greedy or an optimal solver to compute an LSAPe solution $\pi \in \Pi(\mathbf{C})$ and interpret π as a node map whose induced edit cost is returned as an upper bound for GED. Alternatively, given a constant $s > 1$, we suggest to use an optimal LSAPe solver in combination with the enumeration procedure in Ref. 50 in order to generate a set $\Pi_s^*(\mathbf{C}) \subseteq \Pi^*(\mathbf{C})$ of optimal LSAPe solutions with size $|\Pi_s^*(\mathbf{C})| = \min\{s, |\Pi^*(\mathbf{C})|\}$. A tightened upper bound for GED can then be obtained by minimizing the induced edit cost over the solution set $\Pi_s^*(\mathbf{C})$. Using the enumeration procedure in Ref. 50 to compute solution sets $\Pi_s^*(\mathbf{C})$ with $s > 1$ was suggested in Ref. 18, where $\Pi_s^*(\mathbf{C})$'s elements are used as initial solutions for a refinement algorithm based on local search. However, to the best of our knowledge, this technique has never been used for tightening the upper bounds produced by LSAPe based heuristics.

3.2. Classical instantiations

Classical instantiations of the paradigm LSAPe-GED construct the LSAPe instance \mathbf{C} by using local structures rooted at the nodes and distance measures between them. Formally, they define local structure functions $\mathcal{S} : \mathcal{J} \rightarrow \mathfrak{S}$ that map graph-node incidences to elements of a suitably defined space of local structures \mathfrak{S} , and distance measures $d_{\mathfrak{S}} : \mathfrak{S} \times \mathfrak{S} \rightarrow \mathbb{R}_{\geq 0}$ for the local structures. Given input graphs G and H on node sets $V^G = \{u_1, \dots, u_{|V^G|}\}$ and $V^H = \{v_1, \dots, v_{|V^H|}\}$, the LSAPe

10 *D.B. Blumenthal, J. Gamper, S. Bougleux & L. Brun*

| | 1 | 2 | 3 | 4 | 5 |
|---|--------------|--------------|--------------|--------------|--------------|
| 1 | 0.177 | 1.406 | 1.208 | 0.468 | 0.675 |
| 2 | 1.203 | 0.272 | 1.403 | 0.832 | 0.675 |
| 3 | 1.226 | 1.180 | 0.260 | 1.259 | 0.675 |
| 4 | 0.788 | 0.705 | 1.346 | 0.390 | 0.675 |
| 5 | 1.135 | 0.369 | 0.906 | 0.902 | 0.675 |
| 6 | 0.675 | 0.675 | 0.675 | 0.675 | 0 |

Fig. 3. LSAPE instance \mathbf{C} for the graphs shown in Figure 1 constructed by the toy instantiation of LSAPE-GED described in Example 2. Bold-faced cells correspond to the node assignments contained in optimal solution.

instance $\mathbf{C} \in \mathbb{R}^{(|V^G|+1) \times (|V^H|+1)}$ is then defined as $c_{i,k} := d_{\mathfrak{S}}(\mathcal{S}(G, u_i), \mathcal{S}(H, v_k))$, $c_{i,|V^H|+1} := d_{\mathfrak{S}}(\mathcal{S}(G, u_i), \mathcal{S}(H, \epsilon))$, and $c_{|V^G|+1,k} := d_{\mathfrak{S}}(\mathcal{S}(G, \epsilon), \mathcal{S}(H, v_k))$, for all $(i, k) \in [|V^G|] \times [|V^H|]$. This classical strategy for populating \mathbf{C} is adopted by BP,³⁸ STAR,⁵² BRANCH-UNI,⁵⁵ BRANCH,⁷ BRANCH-FAST,⁷ WALKS,²¹ and SUBGRAPH,¹⁵ as well as by the algorithm RING proposed in this paper (Section 5.1). Also the node centrality based heuristics^{41,47} can be subsumed under this model; here, the “local structures” are simply the nodes’ centralities.

Example 2 (Classical Instantiations of LSAPE-GED). Consider a very simple classical instantiation of LSAPE-GED that uses the input graphs’ node labels as its local structures and the node edit costs c_V as the local structure distances. Figure 3 shows the obtained LSAPE instance \mathbf{C} for the graphs G and H shown in Figure 1 under the assumption that c_V is defined as detailed in Example 1. Its optimal solution $\pi := \{(i, i) \mid i \in [5]\}$ selects the bold-faced cells of \mathbf{C} and corresponds to the node map shown in Figure 1. Its LSAPE cost is hence $\mathbf{C}(\pi) = 1.774$, and the induced upper bound for GED equals $c(\pi) = 2.574$.

The formal specification of the paradigm LSAPE-GED allows us to introduce a partial order \succeq_T that orders local structure functions employed by classical instantiations w. r. t. their topological information content (cf. Definition 4). The intuition behind \succeq_T is that a local structure function \mathcal{S}_1 is topologically more informative than another local structure function \mathcal{S}_2 if fixing the local structures $\mathcal{S}_1(G, u)$ implies that also the local structures $\mathcal{S}_2(G, u)$ remain unchanged.

Definition 4 (Partial Order \succeq_T). A local structure function \mathcal{S}_1 is *weakly topologically more informative* than a local structure function \mathcal{S}_2 (in symbols: $\mathcal{S}_1 \succeq_T \mathcal{S}_2$), if and only if $\mathcal{S}_1(G, u) = \mathcal{S}_1(H, v)$ implies $\mathcal{S}_2(G, u) = \mathcal{S}_2(H, v)$. \mathcal{S}_1 is *strictly topologically more informative* than \mathcal{S}_2 ($\mathcal{S}_1 \succ_T \mathcal{S}_2$), if and only if $\mathcal{S}_1 \succeq_T \mathcal{S}_2$ and $\mathcal{S}_2 \not\succeq_T \mathcal{S}_1$.

Proposition 1 states that \succeq_T is indeed a partial order.

Proposition 1. *Let \mathbb{S} be the set of all local structure functions. Then \succeq_T is a*

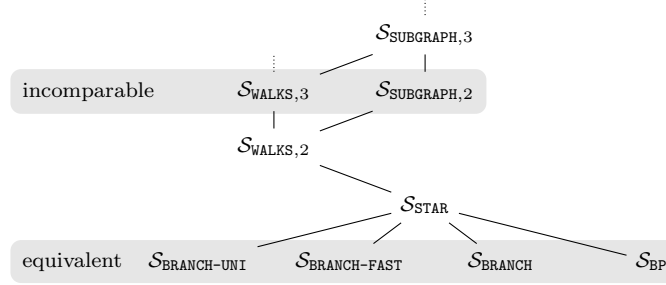


Fig. 4. Hasse diagram induced by strict partial order \succ_T for local structure functions employed by existing instantiations of LSAPG-GED.

partial order on \mathbb{S}/\sim_T , where the equivalence relation \sim_T is defined as $\mathcal{S}_1 \sim_T \mathcal{S}_2 :\Leftrightarrow \mathcal{S}_1 \succeq_T \mathcal{S}_2 \wedge \mathcal{S}_2 \succeq_T \mathcal{S}_1$.

Proof. Reflexivity and anti-symmetry immediately follow from the definitions of \succeq_T and \sim_T . For showing transitivity, let $\mathcal{S}_1, \mathcal{S}_2, \mathcal{S}_3 \in \mathbb{S}$ be local structure functions with $\mathcal{S}_1 \succeq_T \mathcal{S}_2 \succeq_T \mathcal{S}_3$ and $(G, u), (H, v) \in \mathcal{I}$ be graph-node incidences with $\mathcal{S}_1(G, u) = \mathcal{S}_1(H, v)$. From $\mathcal{S}_1 \succeq_T \mathcal{S}_2$, we obtain $\mathcal{S}_2(G, u) = \mathcal{S}_2(H, v)$. Therefore, $\mathcal{S}_2 \succeq_T \mathcal{S}_3$ implies $\mathcal{S}_3(G, u) = \mathcal{S}_3(H, v)$ and hence $\mathcal{S}_1 \succeq_T \mathcal{S}_3$, as required. \square

Proposition 2 below orders existing classical LSAPG-GED instantiations w. r. t. the topological information content of the employed local structure functions. BRANCH-UNI, BRANCH-FAST, BRANCH, and BP are topologically equivalent, because they use the same local structure function \mathcal{S} and differ only w. r. t. the distance measure $d_{\mathcal{G}}$ used on top of it. Among all existing instantiations, SUBGRAPH's local structure function captures most topological information. However, this comes at the price of having to use a distance measure $d_{\mathcal{G}}$ that is not polynomially computable.

Proposition 2. *The strict partial order \succ_T orders local structure functions employed by existing classical LSAPG-GED instantiations as shown in the Hasse diagram in Figure 4.*

Proof. BRANCH-UNI, BRANCH-FAST, BRANCH, and BP all use the same local structure function — namely, branches rooted at the nodes. This implies $\mathcal{S}_{\text{BRANCH-UNI}} \sim_T \mathcal{S}_{\text{BRANCH-FAST}} \sim_T \mathcal{S}_{\text{BRANCH}} \sim_T \mathcal{S}_{\text{BP}}$. The star structures employed by $\mathcal{S}_{\text{STAR}}$ can be viewed as branches that additionally contain the terminal nodes of the edges incident with the root or, alternatively, as the bag of all walks of length 1 starting at the root. This yields $\mathcal{S}_{\text{WALKS},2} \succ_T \mathcal{S}_{\text{STAR}} \succ_T \mathcal{S}_{\text{BRANCH-UNI}}, \mathcal{S}_{\text{BRANCH-FAST}}, \mathcal{S}_{\text{BRANCH}}, \mathcal{S}_{\text{BP}}$. The relations $\mathcal{S}_{\text{SUBGRAPH},L} \succ_T \mathcal{S}_{\text{WALKS},L}$, $\mathcal{S}_{\text{WALKS},L+1} \succ_T \mathcal{S}_{\text{WALKS},L}$, as well as the fact that $\mathcal{S}_{\text{SUBGRAPH},L}$ and $\mathcal{S}_{\text{WALKS},L+1}$ are incomparable directly follow from the definitions of the respective local structure functions. \square

3.3. Machine learning based instantiations

3.3.1. General strategy

Instead of using local structures, LSAPE instances can be constructed with the help of feature vectors associated to good and bad node assignments. This strategy is inspired by the existing algorithms PREDICT⁴² and NGM.¹⁷ However, as detailed in Section 5.3 below, both PREDICT and NGM fall short of completely instantiating it.

Definition 5 (ϵ -Optimal Node Assignments).

A node assignment $(G, H, u, v) \in \mathfrak{A}$ is called ϵ -optimal if and only if it is contained in an ϵ -optimal node map, i. e., if there is a node map $\pi \in \Pi(G, H)$ with $c(\pi) \leq \text{GED}(G, H) \cdot (1 + \epsilon)$ and $(u, v) \in \pi$. \mathfrak{A}_ϵ^* is the set of all ϵ -optimal node assignments. Node assignments contained in $\mathfrak{A} \setminus \mathfrak{A}_\epsilon^*$ are called ϵ -bad.

If machine learning techniques are used for populating \mathbf{C} , feature vectors $\mathcal{F} : \mathfrak{A} \rightarrow \mathbb{R}^d$ for the node assignments have to be defined and a function $p^* : \mathbb{R}^d \rightarrow [0, 1]$ has to be learned, which maps feature vectors $\mathbf{x} \in \mathcal{F}[\mathfrak{A}_\epsilon^*]$ to large and feature vectors $\mathbf{x} \in \mathcal{F}[\mathfrak{A} \setminus \mathfrak{A}_\epsilon^*]$ to small values. Informally, $p^*(\mathbf{x})$ can be viewed as an estimate of the probability that the feature vector \mathbf{x} is associated to an ϵ -optimal node map. Once p^* has been learned, \mathbf{C} is defined as $c_{i,k} := 1 - p^*(\mathcal{F}(G, H, u_i, v_k))$, $c_{i,|V^H|+1} := 1 - p^*(\mathcal{F}(G, H, u_i, \epsilon))$, and $c_{|V^G|+1,k} := 1 - p^*(\mathcal{F}(G, H, \epsilon, v_k))$, for all $(i, k) \in [|V^G|] \times [|V^H|]$.

3.3.2. Choice of machine learning technique

For learning p^* , several strategies can be adopted. Given a set \mathcal{G} of training graphs, one can mimic PREDICT and compute ϵ -optimal node maps $\pi_{G,H}$ for the training graphs. These node maps can be used to generate training data $\mathcal{T} := \{(\mathcal{F}(G, H, u, v), \delta_{(u,v) \in \pi_{G,H}}) \mid (G, H, u, v) \in \mathfrak{A}[\mathcal{G}]\}$, where $\delta_{\text{true}|\text{false}}$ maps **true** to 1 and **false** to 0, and $\mathfrak{A}[\mathcal{G}]$ is the restriction of \mathfrak{A} to the graphs contained in \mathcal{G} . Finally, a kernelized SVC with probability estimates³³ can be trained on \mathcal{T} . Alternatively, one can proceed like NGM, i. e., use \mathcal{T} to train a fully connected feedforward DNN with output from $[0, 1]$, and define p^* as the output of the DNN.

The drawback of these approaches is that some feature vectors are incorrectly labeled as ϵ -bad if there is more than one ϵ -optimal node map. Assume that, for training graphs G and H , there are two ϵ -optimal node maps $\pi_{G,H}$ and $\pi'_{G,H}$ and that the algorithm used for generating \mathcal{T} computes $\pi_{G,H}$. Let (G, H, u, v) be a node assignment such that (u, v) is contained in $\pi'_{G,H} \setminus \pi_{G,H}$. According to Definition 5, (G, H, u, v) is an ϵ -optimal node assignment, but in \mathcal{T} , its feature vector $\mathbf{x} := \mathcal{F}(G, H, u, v)$ is labeled as ϵ -bad.

A straightforward but computationally infeasible way to tackle this problem is to compute all ϵ -optimal node maps for the training graphs. Instead, we suggest to train a one class support vector machine (1-SVM)⁴⁶ with RBF kernel to estimate the support of the feature vectors associated to good node maps. This has the advantage

that, given a set \mathcal{G} of training graphs and initially computed ϵ -optimal node maps $\pi_{G,H}$ for all $G, H \in \mathcal{G}$, we can use training data $\mathcal{T}^* := \{\mathcal{F}(G, H, u, v) \mid (G, H, u, v) \in \mathfrak{A}[\mathcal{G}] \wedge (u, v) \in \pi_{G,H}\}$, which contains only feature vectors associated to ϵ -optimal node assignments and is hence correct even if there are multiple ϵ -optimal node maps.

For the definition of p^* , recall that a 1-SVM with RBF kernel learns a multivariate Gaussian mixture model $\mathcal{M}(\boldsymbol{\alpha}, \gamma) := \sum_{i=1}^{|\mathcal{T}^*|} (\mathbf{1}^\top \boldsymbol{\alpha})^{-1} \alpha_i \mathcal{N}(\mathbf{0}, (2\gamma)^{-1} \mathbf{I})$ for the feature vectors $\mathcal{F}[\mathfrak{A}_\epsilon^*]$ associated to ϵ -optimal node assignments, where α_i is the dual variable associated to the training vector $\mathbf{x}^i \in \mathcal{T}^*$ and $\gamma > 0$ is a tuning parameter. We can hence simply define $p^*(\mathbf{x})$ as the likelihood of the feature vector \mathbf{x} under the model $\mathcal{M}(\boldsymbol{\alpha}, \gamma)$ learned by the 1-SVM, i.e., set $p^*(\mathbf{x}) := ((\gamma/\pi)^{d/2} / \mathbf{1}^\top \boldsymbol{\alpha}) \cdot \left(\sum_{i=1}^{|\mathcal{T}^*|} \alpha_i \exp(-\gamma \|\mathbf{x}^i - \mathbf{x}\|_2^2) \right)$.

4. Rings as Local Structures

In this section, we introduce rings of size L as a new kind of local structures. Subsequently, we show how to construct them. As mentioned above, rings are similar to the subgraph and walks structures used, respectively, by **SUBGRAPH** and **WALKS** in that they capture more topological information than the local structures used by the baseline approaches **BP**, **STAR**, **BRANCH-UNI**, and **BRANCH**. They are hence designed to be used by instantiations of **LSAPE-GED** that aim at computing tight upper bounds on datasets where most information resides in the graphs' topologies. The advantage of rings w. r. t. subgraphs is that rings can be processed in polynomial time, while comparing local subgraphs is polynomial only on graphs with constantly bounded maximum degrees. In comparison to walks, rings have two advantages: Firstly, rings model general edit costs, while walks are designed for constant edit costs. Secondly, walks often contain redundant information, because it can happen that a walk visits nodes and edges multiple times. Since rings consist of disjoint layers, they do not suffer from this problem.

4.1. Rings: definition and properties

We define the rings rooted at the nodes of a graph G as L -sized sequences of layers $\mathcal{L}^G = (N^G, OE^G, IE^G)$, where $N^G \subseteq V^G$ is a subset of the nodes, and $OE^G, IE^G \subseteq E^G$ are subsets of the edges of G . Formally, the space of all L -sized rings for graphs from a domain \mathfrak{G} is defined as $\mathfrak{R}_L := \{(\mathcal{L}_l)_{l=0}^{L-1} \mid \mathcal{L}_l \in \bigcup_{G \in \mathfrak{G}} \mathfrak{L}(G)\}$, where $\mathfrak{L}(G) := \mathcal{P}(V^G) \times \mathcal{P}(E^G) \times \mathcal{P}(E^G)$. Next, we specify a function $\mathcal{R}_L : \mathfrak{J} \rightarrow \mathfrak{R}_L$ which maps a graph-node incidence (G, u) to a ring of size L . For this, we need some terminology: The distance $d_V^G(u, u')$ between two nodes $u, u' \in V^G$ is defined as the number of edges on a shortest path connecting them or as ∞ if they are in different connected components of G . The eccentricity of a node $u \in V^G$ and the diameter of a graph G are defined as $e_V^G(u) := \max_{u' \in V^G} d_V^G(u, u')$ and $\text{diam}(G) := \max_{u \in V^G} e_V^G(u)$, respectively.

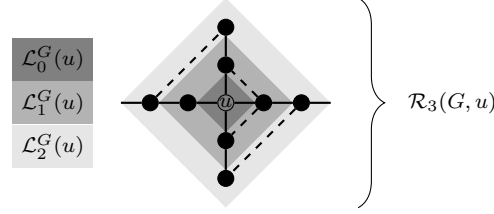


Fig. 5. Visualization of Definition 6. Inner edges are dashed, outer edges are solid. Layers are displayed in different shades of grey.

Definition 6 (Ring). Given a constant $L \in \mathbb{N}_{>0}$, the function $\mathcal{R}_L : \mathcal{J} \rightarrow \mathfrak{R}_L$ maps a graph-node incidence (G, u) to the ring $\mathcal{R}_L(G, u) := (\mathcal{L}_l^G(u))_{l=0}^{L-1}$ rooted at u in G (Figure 5). For the dummy node ϵ , we define $\mathcal{R}_L(G, \epsilon) := ((\emptyset, \emptyset, \emptyset)_l)_{l=0}^{L-1}$. For all other nodes u , $\mathcal{L}_l^G(u) := (N_l^G(u), OE_l^G(u), IE_l^G(u))$ denotes the l^{th} layer rooted at u in G , where:

- (1) $N_l^G(u) := \{u' \in V^G \mid d_V^G(u, u') = l\}$ is the set of nodes at distance l from u .
- (2) $IE_l^G(u) := E^G \cap (N_l^G(u) \times N_l^G(u))$ is the set of inner edges connecting two nodes in the l^{th} layer.
- (3) $OE_l^G(u) := E^G \cap (N_l^G(u) \times N_{l+1}^G(u))$ is the set of outer edges connecting a node in the l^{th} layer to a node in the $(l+1)^{\text{th}}$ layer.

It is easy to see that the ring $\mathcal{R}_1(G, u)$ of a node $u \in V^G$ corresponds to the branch structures used by BP, BRANCH, BRANCH-FAST, and BRANCH-UNI. Further properties of rings and layers are summarized in Remark 1.

Remark 1 (Properties of Rings). Let $u \in V^G$ be a node and $\mathcal{R}_L(G, u) = ((N_l^G(u), OE_l^G(u), IE_l^G(u)))_{l=0}^L$ be the ring of size L rooted at u . Then the following statements follow from the involved definitions:

- (1) The node set $N_l^G(u)$ is empty if and only if $l > e_V^G(u)$, the edge set $IE_l^G(u)$ is empty if $l > e_V^G(u)$, and the edge set $OE_l^G(u)$ is empty if and only if $l > e_V^G(u) - 1$.
- (2) All node sets $N_l^G(u)$ and all edge sets $OE_l^G(u)$ and $IE_l^G(u)$ are disjoint.
- (3) The equalities $\bigcup_{l=0}^{L-1} N_l^G(u) = V^G$ and $\bigcup_{l=0}^{L-1} (OE_l^G(u) \cup IE_l^G(u)) = E^G$ hold for all $u \in V^G$ if and only if $L > \text{diam}(G)$.

Proposition 3 and Figure 6 show how rings relate to existing local structures in terms of topological information content. We see that rings of size at least 2 are strictly topologically more informative than the local structures employed by the baseline instantiations BRANCH-UNI, BRANCH-FAST, BRANCH, BP, and STAR. Moreover, for fixed sizes, rings are incomparable to the bags of walks used by WALKS and strictly topologically less informative than the rooted subgraphs used by SUBGRAPH. Recall, however, that rooted subgraphs cannot be compared in polynomial time and that bags of walks only model constant edit costs. Rings are hence the only

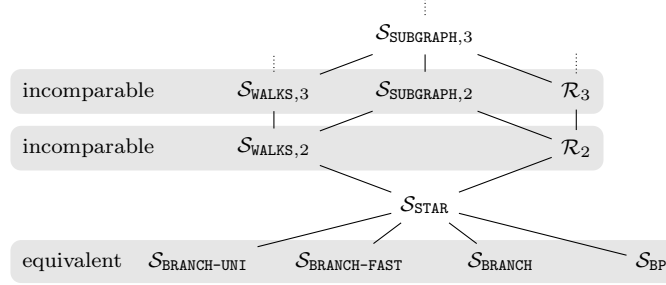


Fig. 6. Hasse diagram induced by strict partial order \succ_T for rings and local structure functions employed by existing instantiations of LSAPG-GED.

generically applicable and polynomially comparable local structures that provably capture more topological information than the baseline structures.

Proposition 3. *The strict partial order \succ_T orders the ring functions \mathcal{R}_L and local structure functions employed by existing classical LSAPG-GED instantiations as shown in the Hasse diagram in Figure 6.*

Proof. Since rings of size 2 are stars plus inner and outer edges in the layer with index 1, we have $\mathcal{R}_2 \succ_T \mathcal{S}_{\text{STAR}} \cdot \mathcal{S}_{\text{WALKS},L} \not\prec_T \mathcal{R}_L$ is implied by the fact that bags of walks are oblivious as to how far the nodes on the walks are away from the root. Conversely, rings do not model how nodes in different layers are connected to each others, which implies $\mathcal{R}_L \not\prec_T \mathcal{S}_{\text{WALKS},L} \cdot \mathcal{R}_{L+1} \succ_T \mathcal{R}_L$, $\mathcal{S}_{\text{SUBGRAPH},L} \succeq_T \mathcal{R}_L$, and the fact that \mathcal{R}_{L+1} and $\mathcal{S}_{\text{SUBGRAPH},L}$ are incomparable directly follow from the involved definitions. \square

4.2. Rings: construction

Figure 7 shows how to construct a ring $\mathcal{R}_L(G, u)$ via breadth-first search. The algorithm maintains the level l of the currently processed layer along with the layer's node and edge sets N , OE , and IE , a vector \mathbf{d} that stores for each node $u' \in V^G$ the distance to the root u , flags $\text{discovered}[e]$ that indicate if the edge $e \in E^G$ has already been discovered by the algorithm, and a FIFO queue open which is initialized with the root u . Throughout the algorithm, $\mathbf{d}[u'] = d_V^G(u, u')$ holds for all nodes u' which have already been added to open , while newly discovered nodes u'' have $\mathbf{d}[u''] = \infty$.

If a node u' is popped from open , we check if its distance is larger than the level l of the current layer. If this is case, we store the current layer, increment l , and clear the node and edge sets N , OE , and IE . Next, we add the node u' to N and iterate through its undiscovered incident edges (u', u'') . We mark (u', u'') as discovered and push the node u'' to open if it has not been discovered yet and its distance to u is less than L . If this distance equals l , (u', u'') is added to the inner edges IE ;

16 *D.B. Blumenthal, J. Gamper, S. Bougleux & L. Brun*

Input: Graph G , node $u \in V^G$, constant $L \in \mathbb{N}_{>0}$.
Output: Ring $\mathcal{R}_L(G, u)$ rooted at u .

```

1  $l \leftarrow 0$ ;  $N \leftarrow \emptyset$ ;  $OE \leftarrow \emptyset$ ;  $IE \leftarrow \emptyset$ ;
2  $\mathcal{R}_L(G, u) \leftarrow ((\emptyset, \emptyset, \emptyset)_l)_{l=0}^{L-1}$ ;  $\text{open} \leftarrow \{u\}$ ;
3  $d[u] \leftarrow 0$ ; for  $u' \in V^G \setminus \{u\}$  do  $d[u'] \leftarrow \infty$ ;
4 for  $e \in E^G$  do  $\text{discovered}[e] \leftarrow \text{false}$ ;
5 while  $\text{open} \neq \emptyset$  do
6    $u' \leftarrow \text{open.pop}()$ ;
7   if  $d[u'] > l$  then
8      $\mathcal{R}_L(G, u)_l \leftarrow (N, OE, IE)$ ;  $l \leftarrow l + 1$ ;
9      $N \leftarrow \emptyset$ ;  $OE \leftarrow \emptyset$ ;  $IE \leftarrow \emptyset$ ;
10   $N \leftarrow N \cup \{u'\}$ ;
11  for  $(u', u'') \in E^G$  do
12    if  $\text{discovered}[(u', u'')]$  then continue;
13     $\text{discovered}[(u', u'')] \leftarrow \text{true}$ ;
14    if  $d[u''] = \infty$  then
15       $d[u''] \leftarrow l + 1$ ;
16      if  $d[u''] < L$  then  $\text{open.push}(u'')$ ;
17    if  $d[u''] = l$  then  $IE \leftarrow IE \cup \{(u', u'')\}$ ;
18    else  $OE \leftarrow OE \cup \{(u', u'')\}$ ;
19  $\mathcal{R}_L(G, u)_l \leftarrow (N, OE, IE)$ ; return  $\mathcal{R}_L(G, u)$ ;

```

Fig. 7. Construction of rings via breadth-first search.

otherwise, it is added to the outer edges OE . Once open is empty, the last layer is stored and the complete ring is returned. Since nodes and edges are processed at most once, the algorithm runs in $O(|V^G| + |E^G|)$ time. The runtime complexity is hence independent of the parameter L . How L affects ring based instantiations of LSAPÉ-GED and how it should be chosen is detailed in Section 5.1.3.

5. Instantiations of LSAPÉ-GED Based on Rings and Machine Learning

In this section, we present two new heuristics for ring based transformations to LSAPÉ: RING (Section 5.1) uses the classical transformation strategy; RING-ML (Section 5.2) employs our new machine learning based approach. We also discuss how the existing machine learning based approaches NGM and PREDICT relate to LSAPÉ-GED (Section 5.3).

5.1. RING: a classical instantiation

RING is a classical instantiation of the paradigm LSAPÉ-GED which uses rings of size L as local structures. Therefore, what remains to be done is to define a distance measure $d_{\mathfrak{R}_L} : \mathfrak{R}_L \times \mathfrak{R}_L \rightarrow \mathbb{R}_{\geq 0}$ for the rings. We will define such a distance measure in a bottom-up fashion: Ring distances are defined in terms of layer distances, which, in turn, are defined in terms of node and edge set distances.

Assume that, for all pairs of graphs $(G, H) \in \mathfrak{G} \times \mathfrak{G}$, we have access to measures $d_{\mathcal{P}(V)}^{G,H} : \mathcal{P}(V^G) \times \mathcal{P}(V^H) \rightarrow \mathbb{R}_{\geq 0}$ and $d_{\mathcal{P}(E)}^{G,H} : \mathcal{P}(E^G) \times \mathcal{P}(E^H) \rightarrow \mathbb{R}_{\geq 0}$ that compute distances between subsets of nodes and edges. Then we can define a layer distance measure $d_{\mathfrak{L}}^{G,H} : \mathfrak{L}(G) \times \mathfrak{L}(H) \rightarrow \mathbb{R}_{\geq 0}$ as

$$d_{\mathfrak{L}}^{G,H}(\mathcal{L}^G, \mathcal{L}^H) := \frac{\alpha_0 d_{\mathcal{P}(V)}^{G,H}(N^G, N^H)}{\max\{|N^G|, |N^H|, 1\}} + \frac{\alpha_1 d_{\mathcal{P}(E)}^{G,H}(IE^G, IE^H)}{\max\{|IE^G|, |IE^H|, 1\}} \\ + \frac{\alpha_2 d_{\mathcal{P}(E)}^{G,H}(OE^G, OE^H)}{\max\{|OE^G|, |OE^H|, 1\}},$$

where $\alpha \in \Delta^2$ is a simplex vector of weights associated to the distances between nodes, inner edges, and outer edges. We normalize by the sizes of the involved node and edge sets in order not to overrepresent large layers. Using the layer distances and a simplex weight vector $\lambda \in \Delta^{L-1}$, we define the ring distance measure as follows:

$$d_{\mathfrak{R}_L}((\mathcal{L}_l^G)_{l=0}^{L-1}, (\mathcal{L}_l^H)_{l=0}^{L-1}) := \sum_{l=0}^{L-1} \lambda_l d_{\mathfrak{L}}^{G,H}(\mathcal{L}_l^G, \mathcal{L}_l^H)$$

Next, we define node and edge set distances $d_{\mathcal{P}(V)}^{G,H}$ and $d_{\mathcal{P}(E)}^{G,H}$. To obtain tight upper bounds for GED, they should be defined such that $d_{\mathfrak{R}_L}(\mathcal{R}_L(G, u), \mathcal{R}_L(H, v))$ is small just in case the node assignment (G, H, u, v) induces a small edit cost. We suggest two strategies that meet this desideratum.

5.1.1. LSAPÉ based node and edge set distances

The first approach uses the edit cost functions c_V and c_E to populate LSAPÉ instances and then defines the distances in terms of the costs of optimal or greedy LSAPÉ solutions. Given node sets $N^G = \{u_1, \dots, u_{|N^G|}\} \subseteq V^G$ and $N^H = \{v_1, \dots, v_{|N^H|}\} \subseteq V^H$, an LSAPÉ instance $\mathbf{C} \in \mathbb{R}^{(|N^G|+1) \times (|N^H|+1)}$ is defined as $c_{i,k} := c_V(\ell_V^G(u_i), \ell_V^H(v_k))$, $c_{i,|N^H|+1} := c_V(\ell_V^G(u_i), \epsilon)$, and $c_{|N^G|+1,k} := c_V(\epsilon, \ell_V^H(v_k))$, for all $(i, k) \in [|N^G|] \times [|N^H|]$. Then, a solution $\pi \in \Pi(\mathbf{C})$ is computed — either optimally in $O(\min\{|N^G|, |N^H|\}^2 \max\{|N^G|, |N^H|\})$ time or greedily in $O(|N^G||N^H|)$ time — and the node set distance $d_{\mathcal{P}(V)}^{G,H}$ between N^G and N^H is defined as $d_{\mathcal{P}(V)}^{G,H}(N^G, N^H) := \mathbf{C}(\pi)$. The edge set distance $d_{\mathcal{P}(E)}^{G,H}$ can be defined analogously.

18 *D.B. Blumenthal, J. Gamper, S. Bougleux & L. Brun*

5.1.2. Multiset based node and edge set distances

Using LSAPe to define $d_{\mathcal{P}(V)}^{G,H}$ and $d_{\mathcal{P}(E)}^{G,H}$ yields fine-grained distance measures but incurs a relatively high computation time. As an alternative, we suggest a faster, multiset intersection based approach which computes a proxy for the LSAPe based distances. For this, the distance between node sets $N^G \subseteq V^G$ and $N^H \subseteq V^H$ is defined as

$$d_{\mathcal{P}(V)}^{G,H} := \delta_{|N^G| > |N^H|} \bar{c}_{del} (|N^G| - |N^H|) + \delta_{|N^G| < |N^H|} \bar{c}_{ins} (|N^H| - |N^G|) \\ + \bar{c}_{sub} (\min\{|N^G|, |N^H|\} - |\ell_V^G[N^G] \cap \ell_V^H[N^G]|),$$

where \bar{c}_{del} , \bar{c}_{ins} , and \bar{c}_{sub} are the average costs of deleting a node in N^G , inserting a node in N^H , and substituting a node in N^G by a differently labeled node in N^H , and $\ell_V^G[N^G]$ and $\ell_V^H[N^H]$ are the multiset images of N^G and N^H under ℓ_V^G and ℓ_V^H .

Since multiset intersections can be computed in quasilinear time,⁵² the dominant operation is the computation of \bar{c}_{sub} which requires $O(|N^G||N^H|)$ time. Again, the edge set distance $d_{\mathcal{P}(E)}^{G,H}$ can be defined analogously. The following Proposition 4 relates the LSAPe based definitions of $d_{\mathcal{P}(V)}^{G,H}$ and $d_{\mathcal{P}(E)}^{G,H}$ to the ones based on multiset intersection and justifies our claim that the latter are proxies for the former.

Proposition 4. *Let $G, H \in \mathfrak{G}$, $N^G \subseteq V^G$, $N^H \subseteq V^H$, and assume that c_V is quasimetric between N^G and N^H , i. e., that $c_V(\ell_V^G(u), \ell_V^H(v)) \leq c_V(\ell_V^G(u), \epsilon) + c_V(\epsilon, \ell_V^H(v))$ holds for all $(u, v) \in N^G \times N^H$. Then the definitions of $d_{\mathcal{P}(V)}^{G,H}(N^G, N^H)$ based on LSAPe and multiset intersection incur the same number of node insertions, deletions, and substitutions. If, additionally, there are constants $c_{del}, c_{ins}, c_{sub} \in \mathbb{R}_{\geq 0}$ such that the equations $c_V(\ell_V^G(u), \ell_V^H(v)) = c_{sub}$, $c_V(\ell_V^G(u), \epsilon) = c_{del}$, and $c_V(\epsilon, \ell_V^H(v)) = c_{ins}$ hold for all $(u, v) \in N^G \times N^H$, the two definitions coincide. For the edge set distances $d_{\mathcal{P}(E)}^{G,H}$, analogous statements hold.*

Proof. Assume w. l. o. g. that $|N^G| \leq |N^H|$, let \mathbf{C} be the LSAPe instance for N^G and N^H constructed as shown in Section 5.1.1, and π be an optimal solution for \mathbf{C} . Since c_V is quasimetric, we know from¹³ that π does not contain deletions and contains exactly $|N^H| - |N^G|$ insertions. This proves the first part of the proposition. If we additionally have constant edit costs between N^G and N^H , $\mathbf{C}(\pi)$ is reduced to the cost of $|N^H| - |N^G|$ insertions plus $c_{sub} = \bar{c}_{sub}$ times the number of non-identical substitutions. This last quantity is provided by $|N^G| - |\ell_V^G[N^G] \cap \ell_V^H[N^G]|$. We thus have $\mathbf{C}(\pi) = \bar{c}_{ins} (|N^H| - |N^G|) + \bar{c}_{sub} (|N^G| - |\ell_V^G[N^G] \cap \ell_V^H[N^G]|)$, as required. The proof for $d_{\mathcal{P}(E)}^{G,H}$ is analogous. \square

5.1.3. Choice of parameters and runtime complexity

In Figure 8, an algorithm is described that, given a set of training graphs \mathcal{G} and node and edge set distances $d_{\mathcal{P}(V)}^{G,H}$ and $d_{\mathcal{P}(E)}^{G,H}$, learns good values for L , α , and λ . First, L is set to an upper bound for the ring sizes and all rings of size L rooted at

- Input:** Set of graphs \mathcal{G} , node and edge set distances $d_{\mathcal{P}(V)}^{G,H}$ and $d_{\mathcal{P}(E)}^{G,H}$, tuning parameter μ .
- Output:** Optimized parameters L , α , λ .
- 1 $L \leftarrow 1 + \max_{G \in \mathcal{G}} |V^G|$;
 - 2 build rings $\mathcal{R}_L(G, u)$ for all $G \in \mathcal{G}$ and all $u \in V^G$;
 - 3 $L \leftarrow 1 + \max_{G \in \mathcal{G}} \text{diam}(G)$; // can be computed in step 2
 - 4 $(\alpha, \lambda) \leftarrow \arg \min \{f_{L,\mu}(\alpha, \lambda) \mid \alpha \in \Delta^2, \lambda \in \Delta^{L-1}\}$;
 - 5 $L \leftarrow 1 + \max \text{supp}(\lambda)$;

Fig. 8. Algorithm for learning the parameters L , α , and λ .

the nodes of the graphs $G \in \mathcal{G}$ are constructed (cf. Figure 7). Next, L is lowered to 1 plus the largest $l < L$ such that there is a graph $G \in \mathcal{G}$ and a node $u \in V^G$ with $\mathcal{R}_L(G, u)_l \neq (\emptyset, \emptyset, \emptyset)$. By Remark 1, this l equals the maximal diameter of the graphs contained in \mathcal{G} . Let $\text{RING}_{L,\alpha,\lambda}(G, H)$ bet the upper bound for $\text{GED}(G, H)$ returned by **RING** if called with parameters L , α and λ , and $\mu \in [0, 1]$ be a tuning parameter that should be small if one wants to optimize for tightness and large if one wants to optimize for runtime. Then, a blackbox optimizer⁴⁵ is called to minimize the objective $f_{L,\mu}(\alpha, \lambda) := \left[\mu + (1 - \mu) \cdot \frac{|\text{supp}(\lambda)| - 1}{\max\{1, L-1\}} \right] \cdot \sum_{(G,H) \in \mathcal{G}^2} \text{RING}_{\alpha,\lambda,L}(G, H)$ over all simplex vectors $\alpha \in \Delta^2$ and $\lambda \in \Delta^{L-1}$. We include $|\text{supp}(\lambda)| - 1$ in the objective, because only levels which are contained in the support of λ (i. e., all levels l with $\lambda_l > 0$) contribute to $d_{\mathfrak{R}_L}$. Hence, only few layer distances have to be computed if $|\text{supp}(\lambda)|$ is small. Once optimized parameters α and λ have been computed, L can be further lowered to $L = 1 + \max \text{supp}(\lambda)$.

Remark 2 (Runtime Complexity of RING). Let $G, H \in \mathfrak{G}$ be graphs, $L \in \mathbb{N}_{\geq 0}$ be a constant, and $\Omega = \mathcal{O}(\min\{\max\{|E^G|, |E^H|\}, \max\{\Delta(G), \Delta(H)\}^L\})$ be the size of the largest node or edge set contained in the rings of G and H , where $\Delta(G)$ is G 's maximum degree. Upon constructing the rings, **RING** requires $\mathcal{O}(\Omega^3 |V^G| |V^H|)$ time to populate its LSAP instance, if LSAP based node and edge set distances are used, and $\mathcal{O}(\Omega^2 |V^G| |V^H|)$ time, if multiset based distances are employed.

5.2. RING-ML: a machine learning based instantiation

If LSAP-GED is instantiated with the help of machine learning techniques, feature vectors associated to the node assignments have to be defined. The heuristic **RING-ML** uses rings of size L to accomplish this task. Formally, **RING-ML** defines a function $\mathcal{F} : \mathfrak{A} \rightarrow \mathbb{R}^{6L+10}$ that maps node assignments to feature vectors with six features per layer and ten global features. Let $(G, H, u, v) \in \mathfrak{A}$ be a node assignment and $\mathcal{R}_L(G, u)$ and $\mathcal{R}_L(H, v)$ be the rings rooted at u in G and at v in H , respectively. For each level $l \in \{0, \dots, L-1\}$, a feature vector $\mathbf{x}^l \in \mathbb{R}^6$ is constructed by comparing the layers $\mathcal{R}_L(G, u)_l = (N_l^G(u), OE_l^G(u), IE_l^G(u))$

20 *D.B. Blumenthal, J. Gamper, S. Bougleux & L. Brun*

and $\mathcal{R}_L(H, v)_l = (N_l^H(v), OE_l^H(v), IE_l^H(v))$ at level l : $\mathbf{x}_0^l := |N_l^G(u)| - |N_l^H(v)|$, $\mathbf{x}_1^l := |OE_l^G(u)| - |OE_l^H(v)|$, $\mathbf{x}_2^l := |IE_l^G(u)| - |IE_l^H(v)|$, $\mathbf{x}_3^l := d_{\mathcal{P}(V)}^{G,H}(N_l^G(u), N_l^H(v))$, $\mathbf{x}_4^l := d_{\mathcal{P}(E)}^{G,H}(OE_l^G(u), OE_l^H(v))$, $\mathbf{x}_5^l := d_{\mathcal{P}(E)}^{G,H}(IE_l^G(u), IE_l^H(v))$.

The first three features compare the layers' topologies. The last three features use node and edge set distances $d_{\mathcal{P}(V)}^{G,H}$ and $d_{\mathcal{P}(E)}^{G,H}$ to express the similarity of the involved node and edge labels. RING-ML also constructs a vector $\mathbf{x}^{G,H} \in \mathbb{R}^{10}$ of ten global features: the number of nodes and edges of G and H , the average costs for deleting nodes and edges from G , the average costs for inserting nodes and edges into H , and the average costs for substituting nodes and edges in G by nodes and edges in H . The complete feature vector $\mathcal{F}(G, H, u, v)$ is then defined as the concatenation of the global features $\mathbf{x}^{G,H}$ and the layer features \mathbf{x}^l .

Remark 3 (Runtime Complexity of RING-ML). Let $G, H \in \mathfrak{G}$ be graphs, $L \in \mathbb{N}_{\geq 0}$ be a constant, and Ω be the size of the largest node or edge set contained in one of the rings of G and H . Then, once all rings have been constructed, RING-ML requires $\mathcal{O}((\Omega^3 + f^{\text{ML}}(1))|V^G||V^H|)$ time to populate its LSAP instance \mathbf{C} if LSAP based node and edge set distances are used, and $\mathcal{O}((\Omega^2 + f^{p^*}(1))|V^G||V^H|)$ time if multiset intersection based distances are employed. $\mathcal{O}(f^{p^*}(n))$ is the complexity of evaluating the probability estimate p^* of the chosen machine learning technique on feature vectors of size n .

5.3. NGM and PREDICT in the context of LSAP-GED

To conclude this section, we summarize the existing machine learning based heuristics NGM and PREDICT, and discuss them in the context of the paradigm LSAP-GED.

NGM assumes the node labels to be real-valued vectors and defines the feature vectors $\mathcal{F}(G, H, u, v) := (\ell_V^G(u), \deg^G(u), \ell_V^H(v), \deg^H(v))$. Hence, no feature vectors for node deletions and insertions can be constructed. Next, NGM trains a DNN to obtain probability estimates for a node assignment being good as described in Section 3.3, and uses these estimates to populate an LSAP (not LSAP) instance. This instance is solved to obtain an upper bound for $\text{GED}(G, H)$ in the case where $|V^G| = |V^H|$. NGM cannot be generalized to the case $|V^G| \neq |V^H|$, because the last row and column of the LSAP instance cannot be populated.

Unlike NGM, PREDICT defines feature vectors that cover node deletions and insertions and are defined for general node and edge labels. PREDICT first calls BP to construct an LSAP instance \mathbf{C} . Next, $\mathcal{F}(G, H, u, v)$ is defined as the concatenation of four global statistics of \mathbf{C} , the node and the edge costs encoded in the cell $c_{i,k}$ that corresponds to the node assignment (G, H, u, v) , and ten statistics of the i^{th} row and the k^{th} column of \mathbf{C} . PREDICT then trains a kernelized SVC without probability estimates to learn a decision function, which is used to predict if a node assignment is ϵ -optimal. PREDICT can hence easily be extended to fully instantiate the paradigm LSAP-GED: we only have to replace the SVC by a DNN or a 1-SVM as detailed in Section 3.3.

6. Experimental Evaluation

We carried out extensive experiments to empirically evaluate the newly proposed algorithms. In Section 6.1, we describe the experimental setup; in Section 6.2, we report the results.

6.1. Setup of the experiments

6.1.1. Compared methods

We tested three variants of RING: RING^{OPT} uses optimal LSAPE for defining the set distances $d_{\mathcal{P}(V)}^{G,H}$ and $d_{\mathcal{P}(E)}^{G,H}$, RING^{GD} uses greedy LSAPE, and RING^{MS} uses the multiset intersection based approach. RING-ML was tested with three different machine learning techniques: SVCs with RBF kernel and probability estimates,⁴² fully connected feedforward DNNs,¹⁷ and 1-SVMs with RBF kernel. We compared to LSAPE based competitors that can cope with non-uniform edit costs: BP, BRANCH, BRANCH-FAST, SUBGRAPH, WALKS, and PREDICT. As WALKS assumes constant edit costs, we slightly extended it by averaging the costs before each run. To handle SUBGRAPH’s exponential complexity, we set a time limit of 1 ms for computing a cell $c_{i,k}$ of its LSAPE instance \mathbf{C} . PREDICT was tested with the same probability estimates as RING-ML. Since some of our test graphs have symbolic labels and not all of them are of the same size, we did not include NGM. For all methods, we varied the number of threads and LSAPE solutions over $\{1, 4, 7, 10\}$ and parallelized the construction of \mathbf{C} . Moreover, we included the local search based algorithm IPFP in the experiments, which is one of the most accurate available GED heuristics but is much slower than instantiations of LSAPE-GED, as detailed in Section 1.1.

6.1.2. Benchmark datasets

We tested on the benchmark datasets PAH, ALKANE, LETTER, and AIDS,³⁷ which are widely used in the research community.^{6–8, 11, 15, 18, 38, 43, 47, 55} Table 2 summarizes some of their properties. LETTER contains graphs that model highly distorted letter drawings, while the graphs in PAH, ALKANE, and AIDS represent chemical compounds. For LETTER, we used the edit costs suggested in Ref. 39, for PAH, ALKANE, and AIDS the edit costs defined in Ref. 1. The graphs contained in PAH and ALKANE have unlabeled nodes, i. e., PAH and ALKANE contain graphs whose information is exclusively encoded in the topologies. LETTER and AIDS graphs have a higher node informativeness.

6.1.3. Synthetic datasets

We also tested on synthetic datasets to evaluate the effect of the node informativeness in a controlled setting. For this, we generated datasets s-MOL- $|\Sigma_V|$, for $|\Sigma_V| \in \{1, 4, 7, 10\}$, and datasets s-ACYCLIC- $|\Sigma_V|$, for $|\Sigma_V| \in \{3, 5, 7, 9\}$. The s-MOL- $|\Sigma_V|$ datasets contain synthetic molecules similar to the ones contained in ALKANE. We

22 *D.B. Blumenthal, J. Gamper, S. Bougleux & L. Brun*

Table 2. Properties of benchmark datasets.

| dataset | avg. $ V^G $ | max. $ V^G $ | avg. $ E^G $ | max. $ E^G $ | $ \Sigma_V $ | classes |
|---------|--------------|--------------|--------------|--------------|--------------|---------|
| AIDS | 15.7 | 95 | 16.2 | 103 | 19 | 2 |
| LETTER | 4.7 | 9 | 4.5 | 9 | ∞ | 15 |
| PAH | 20.7 | 28 | 24.4 | 34 | 1 | 2 |
| ALKANE | 8.9 | 10 | 7.9 | 9 | 1 | 1 |

generated the molecules as pairwise non-isomorphic trees whose sizes were randomly drawn from $\{8, 9, 10, 11, 12\}$. Next, we generated four variants of each molecule — one for each of the four datasets S-MOL-1, S-MOL-4, S-MOL-7, and S-MOL-10 — by randomly drawing node labels from $\Sigma_V = [1]$, $\Sigma_V = [4]$, $\Sigma_V = [7]$, and $\Sigma_V = [10]$, respectively. Edges are unlabeled in all variants. The S-ACYCLIC- $|\Sigma_V|$ datasets were generated similarly. More precisely, S-ACYCLIC-3 contains the real-world molecular graphs from the dataset ACYCLIC, a widely used benchmark dataset with $|\Sigma_V| = 3$ and $|\Sigma_E| = 2$. The datasets S-ACYCLIC-5, S-ACYCLIC-7, and S-ACYCLIC-9 contain variants of the molecules, where the node labels were randomly drawn from $\Sigma_V = [5]$, $\Sigma_V = [7]$, and $\Sigma_V = [9]$. The synthetic datasets are hence constructed such that node label informativeness increases with increasing $|\Sigma_V|$. Since rings are designed for graphs where most information resides in the topologies, we expect the tightness gain of ring based heuristics w. r. t. BP, BRANCH, and BRANCH-FAST to drop with increasing $|\Sigma_V|$.

6.1.4. Meta-parameters and training

For learning the meta-parameters of RING^{OPT}, RING^{GD}, RING^{MS}, SUBGRAPH, and WALKS, and training the DNNs, the SVCs, and the 1-SVMs, we picked a training set $\mathcal{S}_1 \subset \mathcal{D}$ with $|\mathcal{S}_1| = 50$ for each dataset \mathcal{D} . Following Ref. 15, 21, we picked the parameter L of SUBGRAPH and WALKS by minimizing the mean upper bound on \mathcal{S}_1 over $L \in \{1, 2, 3, 4, 5\}$. For choosing the meta-parameters of the RING variants, we set the tuning parameter μ to 1 and initialized our blackbox optimizer with 100 random simplex vectors α and λ . For determining the network structure of the fully connected feedforward DNNs, we carried out 5-fold cross validation, varying the number of hidden layers, the number of neurons per hidden layers, and the activation function at hidden layers over the grid $\{1, \dots, 10\} \times \{1, \dots, 20\} \times \{\text{ReLU}, \text{Sigmoid}\}$. Similarly, we determined the meta-parameters C and γ of the SVC via 5-fold cross-validation over $\{10^{-3}, \dots, 10^3\} \times \{10^{-3}, \dots, 10^3\}$. For the 1-SVM, we set $\gamma = 1/\dim(\mathcal{F})$, where $\dim(\mathcal{F})$ is the number of features. IPFP was used to compute ϵ -optimal node maps, with an empirically determined $\epsilon \approx 0.0423$.³ For balancing the training data \mathcal{T} , we randomly picked only $|\pi|$ node assignments $(u, v) \notin \pi$ for each close to optimal node map π . IPFP’s meta-parameters were set to $\kappa = 40$, $L = 3$, and $\rho = 1/4$ (cf.⁹ for explanations of κ , L , and ρ).

Table 3. Effect of machine learning techniques on RING-ML and PREDICT.

| | RING-ML* | PREDICT ⁴² | RING-ML* | PREDICT ⁴² | RING-ML* | PREDICT ⁴² |
|-------------------|---------------------|-----------------------|-------------------------|-----------------------|------------------------|-----------------------|
| | LETTER | | | | | |
| | avg.upper bound b | | avg.runtime t in sec. | | avg.classif. ratio r | |
| DNN ¹⁷ | 8.24 | 8.19 | 2.99×10^{-4} | 1.48×10^{-4} | 0.20 | 0.22 |
| SVC ⁴² | 6.07 | 6.07 | 6.47×10^{-3} | 2.82×10^{-3} | 0.73 | 0.76 |
| 1-SVM* | 5.68 | 5.22 | 2.58×10^{-3} | 2.07×10^{-3} | 0.81 | 0.81 |
| | PAH | | | | | |
| | avg.upper bound b | | avg.runtime t in sec. | | avg.classif. ratio r | |
| DNN ¹⁷ | 25.29 | 44.03 | 5.69×10^{-3} | 1.23×10^{-3} | 0.64 | 0.56 |
| SVC ⁴² | 31.91 | 36.68 | 7.19×10^{-1} | 3.40×10^{-1} | 0.61 | 0.65 |
| 1-SVM* | 24.55 | 24.55 | 2.12×10^{-1} | 1.14×10^{-1} | 0.71 | 0.71 |

6.1.5. Protocol, test metrics, and implementation

For each dataset \mathcal{D} , we randomly selected a test set $\mathcal{S}_2 \subseteq \mathcal{D} \setminus \mathcal{S}_1$ with $|\mathcal{S}_2| = \min\{100, |\mathcal{D} \setminus \mathcal{S}_1|\}$, and ran each method on each pair $(G, H) \in \mathcal{S}_2 \times \mathcal{S}_2$ with $G \neq H$. We recorded the average runtime in seconds (t), the average value of the returned upper bound for GED (b), and the ratio of graphs which are correctly classified if the returned upper bound is employed in combination with a 1-NN classifier (r). For the experiments on the synthetic datasets, we also recorded the deviation in percent from the upper bound computed by the accurate but slow local search algorithm IPFP (d). Having access to a heuristic ALG that yields tight upper bounds is important, because the tighter the upper bound, the higher the recall if ALG is used to approximately answer queries of the form “given a query graph H , a graph collection \mathcal{G} , and a threshold τ , find all graphs $G \in \mathcal{G}$ with $\text{GED}(G, H) \leq \tau$ ”.

All methods were implemented in C++.⁵ We employed the LSAP solver,¹³ used NOMAD²⁶ as our blackbox optimizer, LIBSVM¹⁶ for implementing SVCs and 1-SVMs, and FANN³⁴ for implementing DNNs. Tests were run on a machine with two Intel Xeon E5-2667 processors with 8 cores and 98 GB of main memory. Sources and datasets are available at <https://github.com/dbblumenthal/gedlib/>.

6.2. Results of the experiments

6.2.1. Effect of machine learning techniques

Table 3 shows the performances of different machine learning techniques when used in combination with the feature vectors defined by RING-ML and PREDICT on the datasets LETTER and PAH (with number of threads and maximal number of LSAP solutions set to 10). Starred techniques are presented in this paper. The results for ALKANE and AIDS are similar and are omitted because of space constraints. The tightest upper bounds and best classification ratios were achieved by 1-SVMs. Using DNNs improved the runtime, but resulted in dramatically worse classification ratios

and upper bounds. Using SVCs instead of 1-SVMs negatively affected all three test metrics. In the following, we therefore only report the results for 1-SVMs and DNNs.

6.2.2. *Effect of number of threads and LSAPÉ solutions*

Figure 9 shows the effects of varying the number of threads and LSAPÉ solutions. Unsurprisingly, slower methods benefited more from parallelization than faster ones. The only exception is WALKS, whose local structure distances require a lot of unparallelizable pre-computing. Computing several LSAPÉ solution tightened the upper bounds of mainly those methods that yielded loose upper bounds if run with only one solution. The outlier of SUBGRAPH on LETTER is due to the fact that SUBGRAPH was run with a time limit on the computation of the subgraph distances; and that the employed subproblem solver behaves deterministically only if run to optimality. Increasing the number of LSAPÉ solutions significantly increased the runtimes of only the fastest algorithms. Computationally expensive LSAPÉ-GED instantiations spend most of the runtime on constructing the LSAPÉ instances. For these methods, the additional time required to enumerate the LSAPÉ solutions is negligible.

6.2.3. *Overall performance on benchmark datasets*

Figure 10 summarizes the overall performances of the compared methods on the four benchmark datasets with the number of threads and maximal number of LSAPÉ solutions fixed to 10. We see that, across all datasets, RING^{OPT} yielded the tightest upper bound among all instantiations of LSAPÉ-GED. RING^{MS}, i.e., the variant of RING which uses the multiset intersection based approach for computing the layer distances, performed excellently, too, as it was significantly faster than RING^{OPT} and yielded only slightly looser upper bounds. The variant RING^{GD} performed worse than RING^{OPT} and RING^{MS}. As expected, the local search algorithm IPFP computed the tightest upper bounds but was around two orders of magnitude slower than the variants of RING.

While PAH and ALKANE contain unlabeled graphs whose information is entirely encoded in the topology, LETTER and AIDS graphs have highly discriminative node labels (cf. column $|\Sigma_V|$ in Table 2). This leads to different results for PAH and ALKANE, on the one hand, and LETTER and AIDS, on the other hand. On LETTER and AIDS, also the baseline approaches BP, BRANCH, and BRANCH-FAST yield upper bounds which are only slightly looser than IPFP’s close to optimal bounds. Consequently, the tightness gains of the RING variants are marginal. For PAH and ALKANE, the outcomes are very different. Here, the baseline approaches computed much looser upper bounds than IPFP and were clearly outperformed by the RING variants. Using rings hence indeed significantly improves LSAPÉ based heuristics on instances which are difficult to solve because the graphs’ topologies are more important than the node labels.

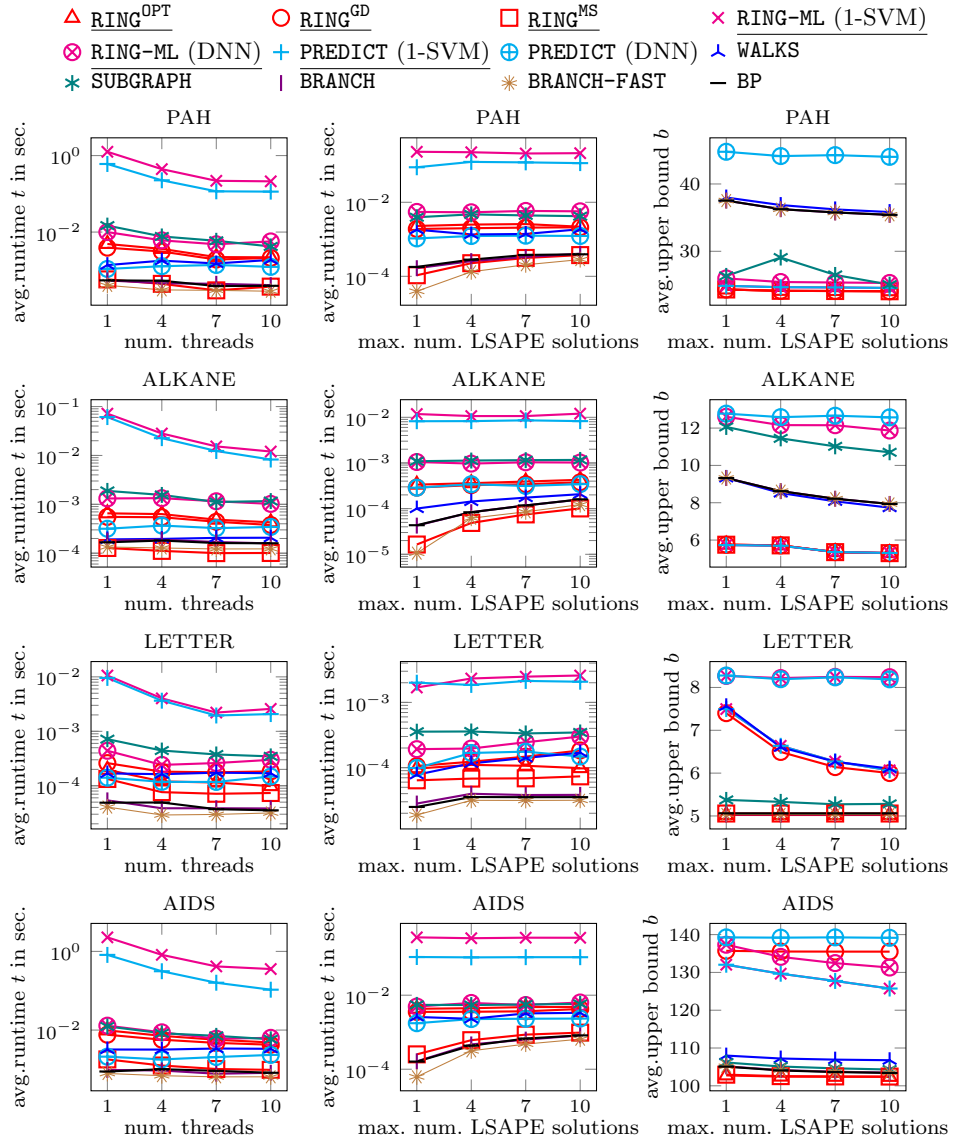


Fig. 9. Number of threads vs.runtimes (first row, maximal number of LSAPF solutions fixed to 10) and maximal number of LSAPF solutions vs.runtimes and upper bounds (second and third row, number of threads fixed to 10). Underlined methods use techniques proposed in this paper.

If run with 1-SVMs with RBF kernels, the machine learning based methods PREDICT and RING-ML performed very similarly in terms of classification ratio and tightness of the produced upper bounds. Both yielded very promising classification

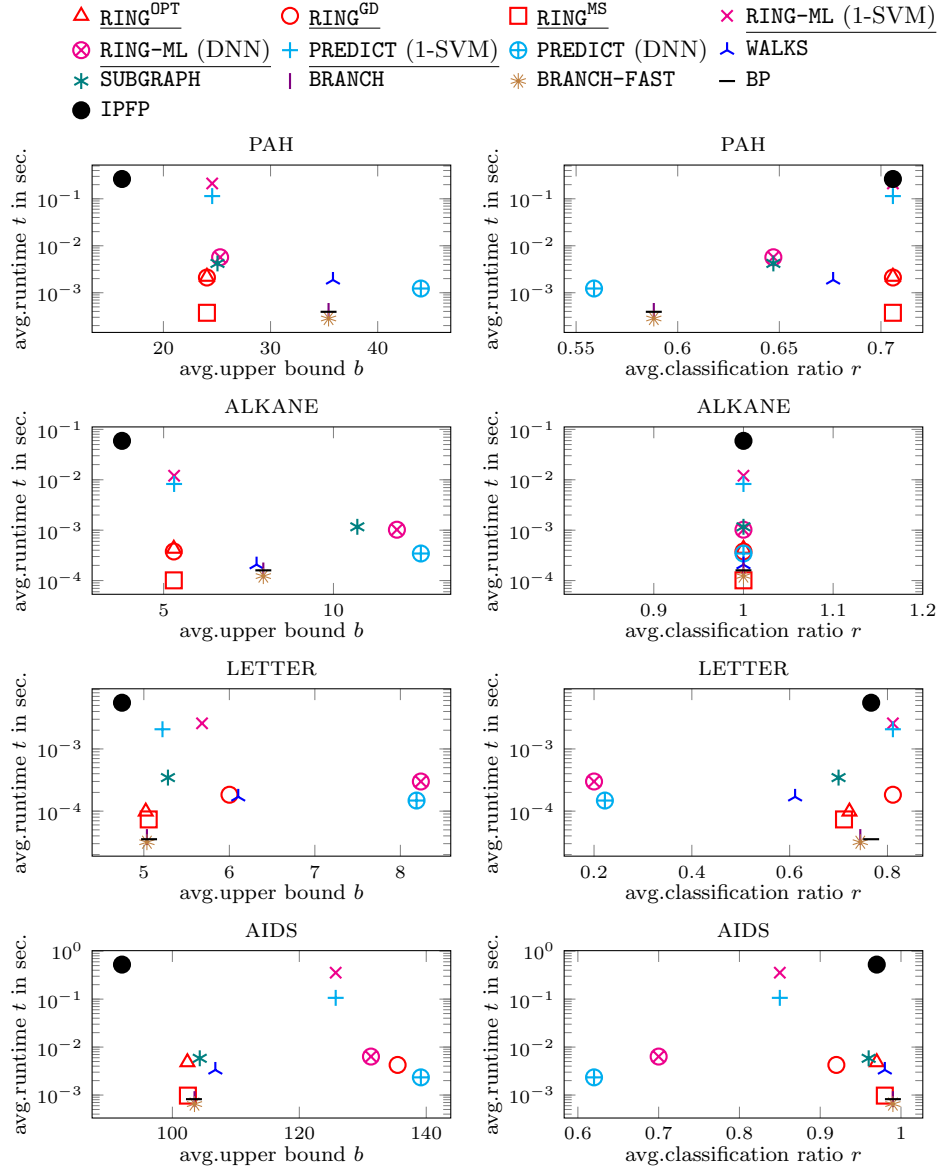


Fig. 10. Runtimes vs. upper bounds and classification ratios with number of threads and maximal number of LSAPe solutions fixed to 10. Underlined methods use techniques proposed in this paper. As ALKANE contains only one graph class, on this dataset, we have $r(\text{ALG}) = 1$ for all algorithms ALG.

ratios on PAH and LETTER, but were not competitive w.r.t. runtime, because, at runtime, $\|\mathbf{x}^i - \mathcal{F}(G, H, u, v)\|_2^2$ has to be computed for each node assignment (G, H, u, v) and each training vector \mathbf{x}^i (cf. Section 3.3.2). Running RING-ML and

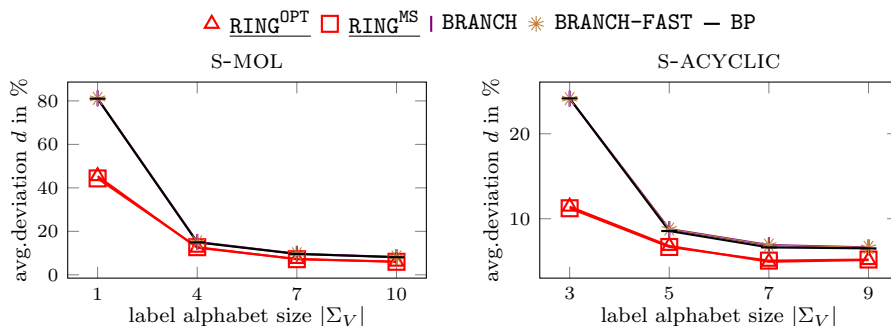


Fig. 11. Effect of node informativeness with number of threads and maximal number of LSAPE solutions fixed to 10. Underlined methods use techniques proposed in this paper. Methods whose curves are not displayed yielded higher deviations or were much slower.

PREDICT with DNNs instead of 1-SVMs dramatically improved the runtimes but led to looser upper bounds and worse classification ratios. If run with DNNs, RING-ML produced tighter upper bounds than PREDICT. Yet, globally, the machine learning based methods were outperformed by classical LSAPE-GED instantiations.

6.2.4. Results for synthetic datasets

Figure 11 shows the results for the synthetic datasets. The curves visualize by how much the upper bounds computed by LSAPE based heuristics deviate from IPFP’s close to optimal upper bounds. Recall that small $|\Sigma_V|$ means that most information resides in the graphs’ topologies. To improve the readability, we only show the curves for RING^{OPT}, RING^{MS}, and the methods BP, BRANCH, and BRANCH-FAST that employ narrow local structures. All other methods yielded looser upper bounds or were much slower.

RING^{OPT} and RING^{MS} performed very similarly and always yielded the best upper bounds. As expected, the tightness gap between RING^{OPT} and RING^{MS}, on the one side, and BP, BRANCH, and BRANCH-FAST, on the other side, was much higher on the datasets S-MOL-1 and S-ACYCLIC-3 than on the datasets S-MOL- $|\Sigma_V|$ and S-ACYCLIC- $|\Sigma_V|$ for $|\Sigma_V| > 3$. The tests on synthetic graphs hence confirms our explanation for the observed results on the benchmark datasets: Using ring based heuristics is especially beneficial if most information is encoded in the graphs’ topologies rather than in the node labels.

6.2.5. Upshot of the results

The experiments yield four take-home messages: Firstly, RING^{OPT} and RING^{MS} are the methods of choice if one wants to compute tight upper bounds for GED on graphs where most information is encoded in the topology but cannot afford to run much slower local search based heuristics such as IPFP. Secondly, one should

always compute several LSAPÉ solutions. This only slightly increases the runtime and at the same time significantly improves the upper bounds of methods that yield loose upper bounds if run with only one LSAPÉ solution. Thirdly, machine learning based LSAPÉ-GED instantiations such as RING-ML and PREDICT should be run with 1-SVMs as suggested in this paper if one wants to optimize for classification ratio and tightness of the produced upper bound, and with DNNs as suggested in Ref. 17 if one wants to optimize for runtime. Fourthly, RING-ML and PREDICT show promising potential but cannot yet compete with classical instantiations of LSAPÉ-GED. If run with 1-SVMs, they are competitive in terms of classification ratio and tightness of the produced upper bound but not in terms of runtime; if run with DNNs, the opposite is the case. The open challenge for future work is therefore to develop new machine learning frameworks that exploit the information encoded in RING-ML's and PREDICT's feature vectors such that the resulting GED heuristics are competitive both w. r. t. quality and w. r. t. runtime behaviour.

7. Conclusions and Future Work

In this paper, we formalized the paradigm LSAPÉ-GED for upper bounding GED via transformations to LSAPÉ and showed how to use machine learning in general in 1-SVMs in particular for this purpose. Moreover, we introduced rings, a new kind of local structures to be used by instantiations of LSAPÉ-GED, and presented the algorithms RING and RING-ML that use rings to instantiate LSAPÉ-GED in a classical way (RING) or via machine learning (RING-ML).

Extensive experiments showed that, while existing instantiations of LSAPÉ-GED struggle with datasets where the information is mainly encoded in the graphs' topologies, RING yields tight upper bounds also on such difficult instances. RING hence closes the gap between existing instantiations of LSAPÉ and accurate but very slow local search algorithms such as IPFP. In other words, RING is the first available GED heuristics which allows to quickly compute reasonably tight upper bounds for GED on difficult instances. In future work, we will seek to boost the performance of RING-ML by using automated feature selection techniques for weighing the importance of the employed local and global features.

References

1. Z. Abu-Aisheh, B. Gaüzere, S. Bogleux, J.-Y. Ramel, L. Brun, R. Raveaux, P. Héroux and S. Adam, Graph edit distance contest 2016: Results and future challenges, *Pattern Recognit.Lett.* **100** (2017) 96–103.
2. Y. Bai, H. Ding, S. Bian, T. Chen, Y. Sun and W. Wang, SimGNN: A neural network approach to fast graph similarity computation, in *WSDM* (2019) pp. 384–392.
3. D. B. Blumenthal, N. Boria, J. Gamper, S. Bogleux and L. Brun, Comparing heuristics for graph edit distance computation, *VLDB J.* **29**(1) (2020) 419–458.
4. D. B. Blumenthal, S. Bogleux, J. Gamper and L. Brun, Ring based approximation of graph edit distance, in *S+SSPR* (2018) pp. 293–303.
5. D. B. Blumenthal, S. Bogleux, J. Gamper and L. Brun, GEDLIB: A C++ library for graph edit distance computation, in *GbRPR* (2019) pp. 14–24.

6. D. B. Blumenthal, É. Daller, S. Bougleux, L. Brun and J. Gamper, Quasimetric graph edit distance as a compact quadratic assignment problem, in *ICPR (2018)* pp. 934–939.
7. D. B. Blumenthal and J. Gamper, Improved lower bounds for graph edit distance, *IEEE Trans.Knowl.Data Eng.* **30**(3) (2018) 503–516.
8. D. B. Blumenthal and J. Gamper, On the exact computation of the graph edit distance, *Pattern Recognit.Lett.* **134** (2020) 46–57.
9. N. Boria, D. B. Blumenthal, S. Bougleux and L. Brun, Improved local search for graph edit distance, *Pattern Recognit.Lett.* **129** (2020) 19–25.
10. N. Boria, S. Bougleux and L. Brun, Approximating GED using a stochastic generator and multistart IPFP, in *S+SSPR (2018)* pp. 460–469.
11. S. Bougleux, L. Brun, V. Carletti, P. Foggia, B. Gaüzère and M. Vento, Graph edit distance as a quadratic assignment problem, *Pattern Recognit.Lett.* **87** (2017) 38–46.
12. S. Bougleux, B. Gaüzère and L. Brun, Graph edit distance as a quadratic program, in *ICPR (2016)* pp. 1701–1706.
13. S. Bougleux, B. Gaüzère, D. B. Blumenthal and L. Brun, Fast linear sum assignment with error-correction and no cost constraints, *Pattern Recognit.Lett.* **134** (2020) 37–45.
14. H. Bunke and G. Allermann, Inexact graph matching for structural pattern recognition, *Pattern Recognit.Lett.* **1**(4) (1983) 245–253.
15. V. Carletti, B. Gaüzère, L. Brun and M. Vento, Approximate graph edit distance computation combining bipartite matching and exact neighborhood substructure distance, in *GbRPR (2015)* pp. 188–197.
16. C.-C. Chang and C.-J. Lin, LIBSVM: A library for support vector machines, *ACM Trans.Intell.Syst.Technol.* **2**(3) (2011) p. 27.
17. X. Cortés, D. Conte, H. Cardot and F. Serratos, A deep neural network architecture to estimate node assignment costs for the graph edit distance, in *S+SSPR (2018)* pp. 326–336.
18. É. Daller, S. Bougleux, B. Gaüzère and L. Brun, Approximate graph edit distance by several local searches in parallel, in *ICPRAM (2018)* pp. 149–158.
19. M. Ferrer, F. Serratos and K. Riesen, A first step towards exact graph edit distance using bipartite graph matching, in *GbRPR (2015)* pp. 77–86.
20. P. Foggia, G. Percannella and M. Vento, Graph matching and learning in pattern recognition in the last 10 years, *Int.J.Pattern Recognit.Artif.Intell.* **28**(1) (2014) 1450001:1–1450001:40.
21. B. Gaüzère, S. Bougleux, K. Riesen and L. Brun, Approximate graph edit distance guided by bipartite matching of bags of walks, in *S+SSPR 2014* pp. 73–82.
22. Gurobi Optimization LLC, *Gurobi Optimizer Reference Manual*, (2018).
23. IBM Cooperation, *IBM ILOG CPLEX Optimization Studio CPLEX User’s Manual*, (2016).
24. D. Justice and A. Hero, A binary linear programming formulation of the graph edit distance, *IEEE Trans.Pattern Anal.Mach.Intell.* **28**(8) (2006) 1200–1214.
25. J. Kim, D. Choi and C. Li, Inves: Incremental partitioning-based verification for graph similarity search, in *EDBT (2019)* pp. 229–240.
26. S. Le Digabel, Algorithm 909: NOMAD: Nonlinear optimization with the MADS algorithm, *ACM Trans.Math.Softw.* **37**(4) (2011) 44:1–44:15.
27. J. Lerouge, Z. Abu-Aisheh, R. Raveaux, P. Héroux and S. Adam, New binary linear programming formulation to compute the graph edit distance, *Pattern Recognit.* **72** (2017) 254–265.
28. J. Lerouge, Z. Abu-Aisheh, R. Raveaux, P. Héroux and S. Adam, Exact graph edit distance computation using a binary linear program, in *S+SSPR (2016)* pp. 485–495.
29. Y. Li, C. Gu, T. Dullien, O. Vinyals and P. Kohli, Graph matching networks for

30 D.B. Blumenthal, J. Gamper, S. Bougleux & L. Brun

- learning the similarity of graph structured objects, in *ICML* (2019) pp. 3835–3845.
30. Z. Li, X. Jian, X. Lian and L. Chen, An efficient probabilistic approach for graph similarity search, in *ICDE* (2018) pp. 533–544.
 31. Y. Liang and P. Zhao, Similarity search in graph databases: A multi-layered indexing approach, in *ICDE* (2017) pp. 783–794.
 32. C.-L. Lin, Hardness of approximating graph transformation problem, in *Algorithms and Computation* (1994) pp. 74–82.
 33. H.-T. Lin, C.-J. Lin and R. C. Weng, A note on Platt’s probabilistic outputs for support vector machines, *Mach.Learn.* **68**(3) (2007) 267–276.
 34. S. Nissen, Implementation of a fast artificial neural network library (FANN), tech. rep., Department of Computer Science, University of Copenhagen (2003).
 35. E. Ozdemir and C. Gunduz-Demir, A hybrid classification model for digital pathology using structural and statistical pattern recognition, *IEEE Trans.Med.Imaging* **32**(2) (2013) 474–483.
 36. K. Riesen, *Structural Pattern Recognition with Graph Edit Distance* (Springer, Cham, 2015).
 37. K. Riesen and H. Bunke, IAM graph database repository for graph based pattern recognition and machine learning, in *S+SSPR* (2008) pp. 287–297.
 38. K. Riesen and H. Bunke, Approximate graph edit distance computation by means of bipartite graph matching, *Image Vis.Comput.* **27**(7) (2009) 950–959.
 39. K. Riesen and H. Bunke, *Graph Classification and Clustering Based on Vector Space Embedding* (World Scientific, Singapore, 2010).
 40. K. Riesen and H. Bunke, Improving bipartite graph edit distance approximation using various search strategies, *Pattern Recognit.* **48**(4) (2015) 1349–1363.
 41. K. Riesen, H. Bunke and A. Fischer, Improving graph edit distance approximation by centrality measures, in *ICPR* (2014) pp. 3910–3914.
 42. K. Riesen and M. Ferrer, Predicting the correctness of node assignments in bipartite graph matching, *Pattern Recognit.Lett.* **69** (2016) 8–14.
 43. K. Riesen, M. Ferrer, A. Fischer and H. Bunke, Approximation of graph edit distance in quadratic time, in *GbRPR* (2015) pp. 3–12.
 44. K. Riesen, A. Fischer and H. Bunke, Improved graph edit distance approximation with simulated annealing, in *GbRPR* (2017) pp. 222–231.
 45. L. M. Rios and N. V. Sahinidis, Derivative-free optimization: a review of algorithms and comparison of software implementations, *J.Global Optim.* **56**(3) (2013) 1247–1293.
 46. B. Schölkopf, J. C. Platt, J. Shawe-Taylor, A. J. Smola and R. C. Williamson, Estimating the support of a high-dimensional distribution, *Neural Comput.* **13**(7) (2001) 1443–1471.
 47. F. Serratos and X. Cortés, Graph edit distance: Moving from global to local structure to solve the graph-matching problem, *Pattern Recognit.Lett.* **65** (2015) 204–210.
 48. M. Stauffer, A. Fischer and K. Riesen, A novel graph database for handwritten word images, in *S+SSPR* (2016) pp. 553–563.
 49. M. Stauffer, T. Tschachtli, A. Fischer and K. Riesen, A survey on applications of bipartite graph edit distance, in *GbRPR* (2017) pp. 242–252.
 50. T. Uno, A fast algorithm for enumerating bipartite perfect matchings, in *ISAAC* (2001) pp. 367–379.
 51. M. Vento, A long trip in the charming world of graphs for pattern recognition, *Pattern Recognit.* **48**(2) (2015) 291–301.
 52. Z. Zeng, A. K. H. Tung, J. Wang, J. Feng and L. Zhou, Comparing stars: On approximating graph edit distance, *Proc.VLDB Endow.* **2**(1) (2009) 25–36.
 53. X. Zhao, C. Xiao, X. Lin, Q. Liu and W. Zhang, A partition-based approach to

- structure similarity search, *Proc. VLDB Endow.* **7**(3) (2013) 169–180.
54. X. Zhao, C. Xiao, X. Lin, W. Zhang and Y. Wang, Efficient structure similarity searches: a partition-based approach, *VLDB J.* **27**(1) (2018) 53–78.
55. W. Zheng, L. Zou, X. Lian, D. Wang and D. Zhao, Efficient graph similarity search over large graph databases, *IEEE Trans. Knowl. Data Eng.* **27**(4) (2015) 964–978.



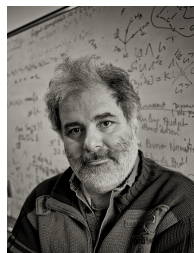
David B. Blumenthal is a postdoctoral fellow at the Chair of Experimental Bioinformatics of the Technical University of Munich, Germany. He received the PhD in computer science from the Free University of Bozen-Bolzano, Italy. His main interests are graph-based data management and algorithmic techniques for network and systems medicine.



Johann Gamper is a full professor at the Faculty of Computer Science of the Free University of Bozen-Bolzano, Italy. He received the PhD in Computer Science from the RWTH Aachen, Germany. His main interests are database technologies for processing temporal and spatial data, data warehousing, and approximate query answering.



Sébastien Bogleux is an associate professor at UNICAEN, ENSICAEN, CNRS, GREYC, Normandie Université, Caen, France. He received the PhD in computer science from the Université de Caen Normandie, France. His main interests are image processing and analysis as well as graph matching and graph similarity search.



Luc Brun is a full professor at ENSICAEN, CNRS, GREYC, Normandie Université, Caen, France. He received the PhD in computer science from the Université Bordeaux I, France. His main research interests are color image segmentation, combinatorial maps, pyramidal data structures, and metrics on graphs.